Clonal expansion of $CD4^+$ cytotoxic T lymphocytes in patients with IgG_4-related disease

Hamid Mattoo, PhD,[a]* Vinay S. Mahajan, MBBS, PhD,[a]* Takashi Maehara, DDS, PhD,[a,b] Vikram Deshpande, MD,[a] Emanuel Della-Torre, MD,[a] Zachary S. Wallace, MD,[a] Maria Kulikova, BS,[a] Jefte M. Drijvers, MD,[a] Joe Daccache, BS,[a] Mollie N. Carruthers, MD,[a] Flavia Castellino, MD,[a] James R. Stone, MD, PhD,[a] John H. Stone, MD, MPH,[a] and Shiv Pillai, MBBS, PhD[a] *Boston, Mass, and Fukuoka, Japan*

Background: IgG_4-related disease (IgG_4-RD) is a systemic condition of unknown cause characterized by highly fibrotic lesions with dense lymphoplasmacytic infiltrates. $CD4^+$ T cells constitute the major inflammatory cell population in IgG_4-RD lesions.

Objective: We used an unbiased approach to characterize $CD4^+$ T-cell subsets in patients with IgG_4-RD based on their clonal expansion and ability to infiltrate affected tissue sites.

Methods: We used flow cytometry to identify $CD4^+$ effector/memory T cells in a cohort of 101 patients with IgG_4-RD. These expanded cells were characterized by means of gene expression analysis and flow cytometry. Next-generation sequencing of the T-cell receptor β chain gene was performed on $CD4^+SLAMF7^+$ cytotoxic T lymphocytes (CTLs) and $CD4^+GATA3^+$ T_H2 cells in a subset of patients to identify their clonality. Tissue infiltration by specific T cells was examined by using quantitative multicolor imaging.

Results: $CD4^+$ effector/memory T cells with a cytolytic phenotype were expanded in patients with IgG_4-RD. Next-generation sequencing revealed prominent clonal expansions of these $CD4^+$ CTLs but not $CD4^+GATA3^+$ memory T_H2 cells in patients with IgG_4-RD. The dominant T cells infiltrating a range of inflamed IgG_4-RD tissue sites were clonally expanded $CD4^+$ CTLs that expressed SLAMF7, granzyme A, IL-1β, and TGF-β1. Clinical remission induced by rituximab-mediated B-cell depletion was associated with a reduction in numbers of disease-associated $CD4^+$ CTLs.

Conclusions: IgG_4-RD is prominently linked to clonally expanded IL-1β– and TGF-β1–secreting $CD4^+$ CTLs in both peripheral blood and inflammatory tissue lesions. These active, terminally differentiated, cytokine-secreting effector $CD4^+$ T cells are now linked to a human disease characterized by chronic inflammation and fibrosis. (J Allergy Clin Immunol 2016;■■■:■■■-■■■.)

Key words: *Fibrosis, IgG_4-related disease, IgG_4, $CD4^+$ cytotoxic T cells, T_H2 cells, rituximab, IL-1β*

IgG_4-related disease (IgG_4-RD) is a chronic inflammatory syndrome with a poorly understood pathogenesis. This disease can affect virtually every organ system of the body and is characterized by tumefactive lesions, storiform fibrosis, obliterative phlebitis, and the presence of IgG_4-secreting plasma cells in affected tissues.[1-3] IgG_4 itself is generally considered a noninflammatory immunoglobulin because of its limited ability to fix complement and bind activating Fc receptors.[4,5] There is very limited evidence that the autoantibodies described thus far are of the IgG_4 subclass, and it is unclear whether they are involved in disease pathogenesis.[6] On the other hand, T cells are the most abundant cells in the lymphoplasmacytic infiltrate in IgG_4-RD lesions and are thought to be the drivers of IgG_4-RD pathogenesis.[2,3]

The analysis of circulating T_H1 and T_H2 cells has led to conflicting results in patients with IgG_4-RD. One study reported a T_H1 skew in peripheral blood T cells in patients with autoimmune pancreatitis, whereas other studies on IgG_4-related sialadenitis showed an increase in numbers of cells expressing T_H2 cytokines in peripheral blood.[7-10] Some T_H2-type cytokines, as well as M2 macrophages, have been found in IgG_4-RD lesions, suggesting that this disease can be caused by T_H2 cells.[11] We have recently reported that atopic manifestations are seen in about 40% of patients with IgG_4-RD, a proportion that is within the range seen in the population at large.[12] We also performed studies on GATA-3–expressing circulating T_H2 cells in patients with IgG_4-RD. Circulating $GATA\text{-}3^+$ IL-4–, IL-5–, and IL-13–secreting T_H2 cells were only found in patients with IgG_4-RD with a history of atopy.[13]

Fibrosis is a prominent feature of many chronic inflammatory disorders, including rheumatoid arthritis, systemic sclerosis, systemic lupus erythematosus, and IgG_4-RD, among others. Many distinct triggers are known to contribute to fibrosis, but a detailed understanding of this pathologic process has proved elusive.[14] Both innate and adaptive immune mechanisms can drive fibrotic responses,[15] but it is unclear what constitutes the tipping point between physiologic wound healing and pathologic fibrosis. Activated macrophages secrete cytokines, such as TNF-α

From [a]Massachusetts General Hospital, Harvard Medical School, Boston, and [b]the Section of Oral and Maxillofacial Oncology, Division of Maxillofacial Diagnostic and Surgical Sciences, Fukuoka.

*These authors contributed equally to this work.

Supported by grants U19-AI110495 and AI 113163 from the National Institutes of Health (NIH). The Massachusetts General Hospital flow core is supported by grant S10RR023440 from the NIH.

Disclosure of potential conflict of interest: V. S. Mahajan has received research support from the National Institutes of Health (NIH; K08 award). F. Castellino has received research support from the NIH and NIAMS (K08 award). J. R. Stone has received consultancy fees and research support from Roche (Genentech). S. Pillai has received research and travel support from the NIH, has received consultancy fees from Genentech, is an unpaid board member for Sialix and Abide, and has received lecture fees for lectures at academic institutions. The rest of the authors declare that they have no relevant conflicts of interest.

Received for publication September 11, 2015; revised November 30, 2015; accepted for publication December 14, 2015.

Corresponding author: Shiv Pillai, MBBS, PhD, Ragon Institute of Massachusetts General Hospital, MIT and Harvard, 400 Tech Square, Cambridge, MA 02139. E-mail: pillai@helix.mgh.harvard.edu. Or: John H. Stone MD, MPH, Rheumatology Unit, Yawkey 2, Massachusetts General Hospital, 55 Fruit St, Boston, MA 02114. E-mail: jhstone@partners.org.

0091-6749/$36.00

© 2016 American Academy of Allergy, Asthma & Immunology

http://dx.doi.org/10.1016/j.jaci.2015.12.1330

Abbreviations used
CTL: Cytotoxic T lymphocyte
Eomes: Eomesodermin
Foxp3: Forkhead box protein 3
IgG_4-RD: IgG_4-related disease
MyD88: Myeloid differentiation primary response gene–88
Runx3: Runt-related transcription factor 3
T-bet: T-box transcription factor
TCR: T-cell receptor
T_{EM}: Effector/memory T
ThPOK: T_H-inducing POZ/Krueppel-like factor

and IL-1β, which activate fibroblasts and induce overproduction of extracellular matrix proteins.[15] In the murine model of bleomycin-induced pulmonary fibrosis, inflammasome activation and IL-1 receptor/myeloid differentiation primary response gene–88 (MyD88) signaling are critical aspects of the profibrotic activity of IL-1β.[16] Transient expression of IL-1β alone in the rat lung has been shown to result in tissue damage and progressive fibrosis.[17] Transgenic overexpression of IL-1β in the murine pancreas also results in fibrotic pancreatitis.[18]

Numerous studies have implicated the type 2 cytokines IL-4, IL-5, and IL-13 in driving progressive fibrosis.[19] IL-4 can directly induce mouse and human fibroblasts to synthesize extracellular matrix proteins.[19-21] IL-13, which is secreted by T_H2 cells, mediates fibrotic remodeling in a TGF-β1–dependent or independent manner in experimental lung fibrosis and might contribute to the pathogenesis of idiopathic pulmonary fibrosis, systemic sclerosis, dermatitis-induced skin fibrosis, and liver fibrosis associated with persistent infections.[22-27] M2 macrophages that have been triggered by IL-4 and IL-13 can induce other cells to produce IL-4, IL-10, IL-13, and TGF-β1 and thus contribute to fibrosis. M2 macrophages involved in wound healing also secrete large amounts of TGF-β1,[28] a cytokine that has also been linked to the genesis of fibrosis. Although fibrosis is generally linked to what is presumably the uncontrolled activity of T_H2 cells, M2 macrophages, and fibroblasts, the prominent role in fibrosis of IL-1β, a cytokine typically made by M1 macrophages, suggests that such T_H2-biased models might be applicable to a subset of fibrotic diseases. The presumption that a number of fibrotic diseases have an underlying T_H2 origin might be an oversimplification of an otherwise complex and poorly understood pathogenic process.

Because expansions of circulating T_H2 cells were not observed in patients with IgG_4-RD without atopy, we undertook an unbiased approach using next-generation sequencing to study the clonality of effector $CD4^+$ T cells in patients with active untreated IgG_4-RD. Our goal was to identify any specific $CD4^+$ effector subpopulation that is clonally expanded in subjects with this disease. We report here that $CD4^+$ T cells with a cytotoxic T-lymphoid phenotype are clonally expanded in patients with IgG_4-RD. Furthermore, these unusual $CD4^+$ T cells can synthesize and secrete IFN-γ, IL-1β, and TGF-β1 after T-cell receptor (TCR) or Toll-like receptor triggering. In addition to these cells being expanded in the blood, they are also found as the dominant $CD4^+$ T-cell population within diseased tissue sites, where they also synthesize cytokines. Their numbers decrease concomitantly with a clinical response to rituximab therapy, suggesting a contributory role for these $CD4^+SLAMF7^+$ cytotoxic T cells in the pathogenesis of this systemic fibrotic disease. We have also observed $CD4^+$ cytotoxic T lymphocyte (CTL) expansions in a smaller cohort with systemic sclerosis. Therefore our data suggest that IFN-γ–, IL-1β–, and TGF-β–secreting $CD4^+$ CTLs contribute to the pathogenesis of IgG_4-RD and are likely to be of broader relevance in other inflammatory fibrotic disorders.

METHODS

Patients

We evaluated peripheral blood from 101 patients with IgG_4-RD and selected tissue samples from a subset of those followed at the Massachusetts General Hospital. This study was approved by the Partners Institutional Review Board. All subjects provided written informed consent. Data pertaining to demographics, prior treatment, and laboratory findings at baseline evaluations were derived from the Massachusetts General Hospital Autoimmune Disease Center of Excellence for IgG_4-RD and the medical record. All patients had biopsy specimens obtained from at least 1 organ that were reviewed and confirmed at our center. For certain analyses, only patients with active untreated disease at sampling were included. Confirmation of the IgG_4-RD diagnosis was predicated on both specific histopathologic features and an increased number of $IgG4^+$ plasma cells (or increased $IgG4^+/IgG^+$ ratio) in affected tissues.[29] Data from patients with IgG_4-RD were compared with those from 35 healthy control subjects (age range, 32-70 years).

Tissue sections from 5 patients with IgG_4-related dacryoadenitis and sialadenitis (ie, IgG_4-related Mikulicz disease; mean age, 68.6 ± 4.12 years) and 5 patients with Sjögren syndrome (mean age, 50.8 ± 9.14 years) obtained from the Department of Oral and Maxillofacial Surgery, Kyushu University Hospital, Fukuoka, Japan, were also studied.

A subset of 74 patients with IgG_4-RD who met the definitions of the European Academy of Allergy and Clinical Immunology[30] were categorized based on their atopic history (see Table E1 in this article's Online Repository at www.jacionline.org). Seventeen patients with systemic sclerosis (age range, 24-85 years; median, 51 years; see Table E2 in this article's Online Repository at www.jacionline.org) were also chosen for this study.

Flow cytometric methods

See the Methods section in this article's Online Repository at www.jacionline.org for detailed laboratory methods. Briefly, flow cytometry was performed by incubating cells in staining buffer (BioLegend, San Diego, Calif) containing optimized concentrations of fluorochrome-conjugated antibodies. Surface staining was performed at 4°C for 30 minutes. For intracellular staining of transcription factors (T-box transcription factor [T-bet], GATA-3, and forkhead box protein 3 [Foxp3]), cytokines (IFN-γ and IL-4), and cytolytic molecules (granzyme B and perforin), cells were fixed and permeabilized with the Foxp3 staining kit (eBioscience, San Diego, Calif), according to the manufacturer's guidelines. Cells were then stained in permeabilization buffer at 4°C for 45 minutes. Stained samples were analyzed on a BD LSR II and sorted on a BD FACSAria II (BD Biosciences, San Jose, Calif).

Methods for next-generation sequencing

Next-generation sequencing analysis of the TCR Vβ repertoire was undertaken with the immunoSEQ platform (Adaptive Biotechnologies, Seattle, Wash), which was designed to target an output of 200,000 assembled output sequences.[31,32]

Gene expression analysis

The nCounter human immunology panel (NanoString Technologies, Seattle, Wash) was used to quantify the gene expression of effector/memory T (T_{EM}) $CD4^+$ cells. Targets were reverse transcribed and preamplified for 14 cycles by using the standard multiplexed target enrichment protocol for 458 immunology-related target genes that were previously validated to yield a linear response. The amplified products were hybridized in solution to color-coded nCounter probes, captured on an nCounter Cartridge for high-resolution digital scanning, and analyzed on the GEN2 Digital Analyzer.

Detailed methodology is included in the Methods section in this article's Online Repository at www.jacionline.org.

RESULTS

Clinical data

Clinical data on the 101 patients with IgG_4-RD are shown in Table I. Of the 101 patients, 61.4% were male, and 75% were of European descent. The average age of disease onset was 51.63 ± 15.3 years. About 53.5% patients had increased serum IgG_4 levels at baseline. Our cohort of patients with IgG_4-RD represented untreated patients with diverse disease presentation, with some patients having a localized single-organ disease (eg, salivary gland involvement and lung disease), and others having a more systemic multiorgan disease (eg, pancreas, kidney, lung, and skin). As reported earlier, around 45% of patients with IgG_4-RD had a history of atopy (see Table E1).[12]

TABLE I. Overview of patients with IgG_4-RD studied

Age at initial evaluation (y), mean ± SD	56.31 ± 13.9
Age at disease onset (y), mean ± SD	51.63 ± 15.3
Male sex (%)	61.4
Race/ethnicity (%)	
White	75
Black	6
Asian	11
Hispanic	6
Middle Eastern	2
Serum IgG_4 (mg/dL), median (IQR)*	147.5 (60.3-387)
Increased serum IgG_4 level at baseline (%)*	53.5
No. of organs affected, mean ± SD	2.3 ± 1.4
Organ involvement (%)	
Type 1 IgG_4-related pancreatitis	18.8
Submandibular/parotid gland disease	38.6
Orbital disease†	19.8
Lymphadenopathy	34.7
Retroperitoneal fibrosis	14.9
Tubulointerstitial nephritis	11.9
Pulmonary disease	19.8

*Among those with active disease.
†Including lacrimal gland involvement (dacryoadenitis).

Effector memory T cells with cytolytic and myeloid features are expanded in patients with IgG_4-RD

We have previously reported that T_H2 cells are seen in the circulation only in a subset of patients with IgG_4-RD with concomitant atopic disease.[13] We corroborated these findings on atopic and nonatopic patients with IgG_4-RD in this larger cohort of patients with IgG_4-RD (see Fig E1 in this article's Online Repository at www.jacionline.org). We sought to investigate patients with IgG_4-RD with active disease in an unbiased way by looking for the presence of $CD4^+$ T-cell populations that have an effector/memory phenotype, presumably resulting from persistent antigenic stimulation.[33,34] We initially performed in-depth studies on 4 patients with active untreated IgG_4-RD. Although all 4 had biopsy-proved IgG_4-RD, their clinical features differed substantially. Patient P2 had lung and kidney involvement, patient P12 presented with submandibular gland disease with lymph node involvement, patient P19 had lesions in the pancreas and submandibular glands and also had retroperitoneal fibrosis, and patient P25 had widespread disease with involvement of the lacrimal glands; parotid, sublingual, and submaxillary glands; kidneys; lungs; skin; and prostate. We observed a striking increase in the proportion and number of $CD4^+CD27^{lo}CD62L^{lo}$ T cells in all 4 patients (Fig 1, *A*). $CD4^+CD27^{lo}CD62L^{lo}$ cells are all $CD45RO^+$ (see Fig E2 in this article's Online Repository at www.jacionline.org) and represent $CD4^+$ T_{EM} cells, which presumably arise from persistent exposure to autoantigens or environmental antigens.[33,35] The presence of regulatory T cells in tissue lesions has been documented in patients with IgG_4-related pancreatitis, sialadenitis, and cholangitis.[7,9,35] However, we observed only a marginal increase in numbers of circulating regulatory T cells that were identified as $CD4^+CD45RO^+CD39^+CD25^+Foxp3^+$ cells in our cohort of patients with IgG_4-RD; this difference was not statistically significant when compared with control subjects (see Fig E3 in this article's Online Repository at www.jacionline.org). Given the significant increase in numbers of $CD4^+$ T_{EM} cells in patients with IgG_4-RD compared with healthy control subjects (Fig 1, *B*), we decided to characterize these cells further and investigate their abundance and potential pathogenic role in patients with IgG_4-RD.

We profiled the expression of a selected panel of genes in this expanded pool of $CD4^+$ T_{EM} cells in the 4 patients described above. Similar gene expression profiles were seen in all 4 patients (Fig 1, *C*). A modified T_H1 gene signature was observed, with increased expression of the transcription factor T-bet along with coexpression of genes encoding 2 SLAM family members, SLAMF7 and 2B4. A number of genes encoding cytolytic proteins, including perforin, granzyme A, granzyme B, and granulysin, were also expressed at high levels. Moreover, these T cells exhibited a distinct myeloid signature with increased expression of genes encoding CD11b, CMKLR1, IL-1β, and CCL4.

Disease-related T_{EM} cells are functional cytolytic cells

The expression of many of the differentially expressed genes in T_{EM} cells was validated at the protein level by using flow cytometry, and a large proportion of the expanded $CD4^+$ T_{EM} cells in PBMCs of diseased patients coexpressed SLAMF7, perforin, granzyme B, and T-bet (Fig 2, *A*). The above markers were also found to be coexpressed in a single expanded clone identified by using the corresponding TCR Vβ–specific antibody, suggesting that the expanded clones represent a uniformly differentiated subpopulation that can be tracked by the expression of SLAMF7 and T-bet (Fig 2, *B*). These cells appear to be phenotypically identical to previously reported $CD4^+$ CTLs seen in patients with chronic viral infections.[11,36] These clonally expanded $CD4^+$ CTLs maintained their phenotype *in vitro* when cultured in the presence of anti-CD3/anti-CD28 beads and recombinant human IL-2 (20 ng/mL, see Fig E4 in this article's Online Repository at www.jacionline.org).

The $CD4^+$ CTLs seen in patients with IgG_4-RD bear a striking resemblance to the cytotoxic $CD4^+$ T lymphocytes reported in mice in the context of chronic antigen stimulation.[37] The development of these cells in mice is associated with gain of Eomesodermin (Eomes) and runt-related transcription factor 3 (Runx3) and loss of T_H-inducing POZ/Krueppel-like factor (ThPOK) expression.[37] Like murine $CD4^+$ CTLs, $CD4^+SLAMF7^+$ T cells from patients with IgG_4-RD exhibited decreased levels of ThPOK and increased expression of Runx3 when compared with $CD4^+CD45RA^+$ naive cells and $CD4^+CD45RO^+$ memory cells from healthy control subjects (Fig 2, *C*). These cells also express surface CD8α, as has been

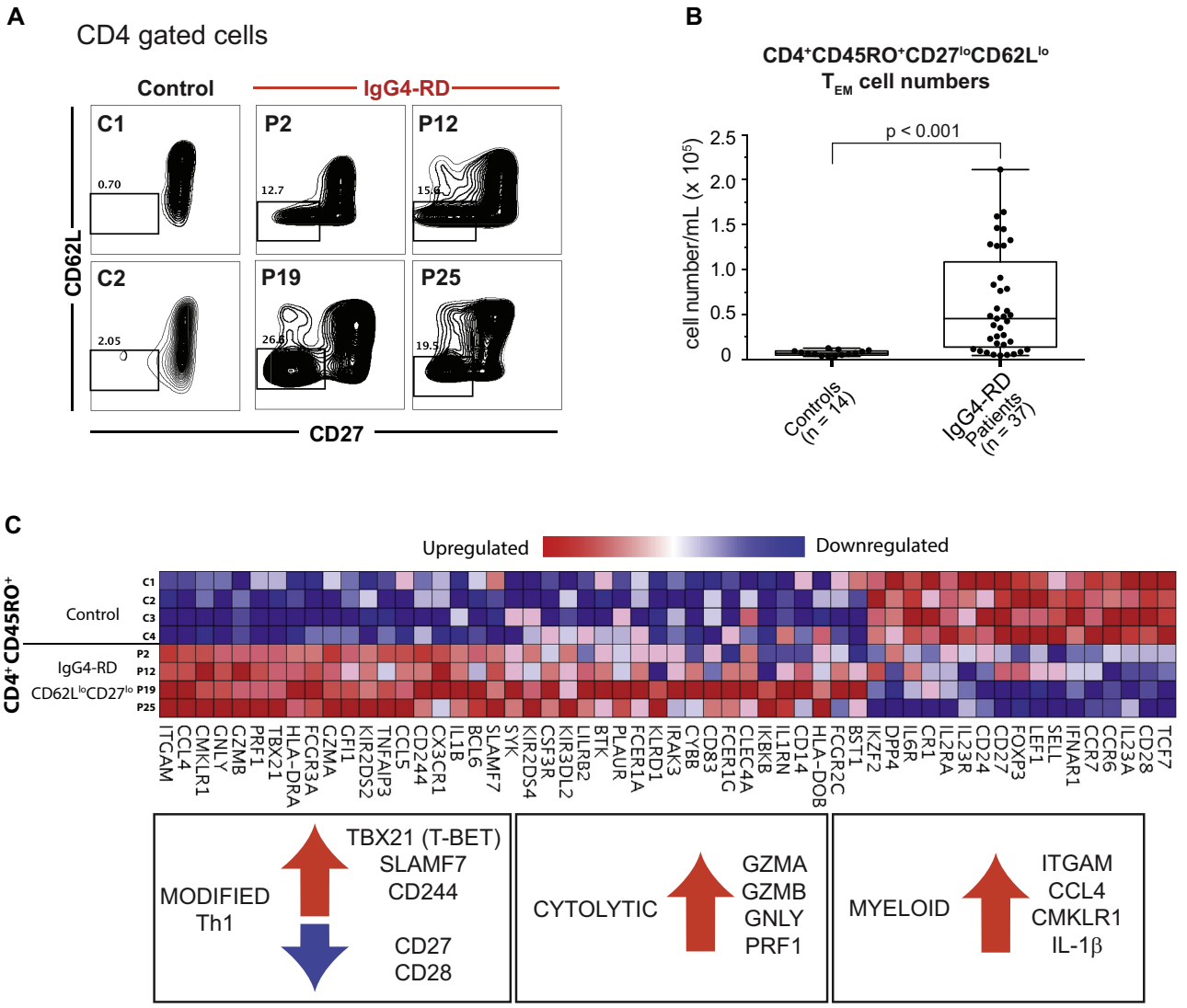


FIG 1. Expansions of T_{EM} cells with a cytolytic phenotype in patients with IgG_4-RD. **A,** $CD4^+CD62L^{lo}CD27^{lo}$ T_{EM} cells in 2 nonatopic (patients P2 and P19) and 2 atopic (patients P12 and P25) patients with IgG_4-RD and 2 representative healthy control subjects. **B,** $CD4^+CD45RO^+CD62L^{lo}CD27^{lo}$ T_{EM} cells in peripheral blood of patients with IgG_4-RD. The *box plot* displays 25th to 75th percentiles. *P* values are based on the Mann-Whitney test. **C,** Heat map depicting differentially expressed immune-related genes in T_{EM} cells from 4 patients with IgG_4-RD compared with $CD4^+CD45RO^+$ T cells from 4 healthy control subjects. Upregulated genes representing modified T_H1, cytolytic, and myeloid signatures are highlighted.

reported in mice (see Fig E5 in this article's Online Repository at www.jacionline.org).[37]

These $CD4^+SLAMF7^+$ T cells have potent cytolytic function; on *in vitro* stimulation with anti-CD3, these cells undergo degranulation, as inferred from the surface expression of CD107a (Fig 2, *D*), and exhibit cytotoxic activity against allogeneic EBV-transformed B-cell targets (Fig 2, *E*, and see Fig E6 in this article's Online Repository at www.jacionline.org).

Circulating $CD4^+SLAMF7^+$ CTLs exhibit large clonal expansions, whereas $CD4^+GATA3^+$ T_H2 cells in patients with IgG_4-RD are clonally diverse

To identify potentially pathogenic subsets of $CD4^+$ T_{EM} cells that were clonally expanded in response to a potential antigen, we analyzed their TCRβ chain gene rearrangements using next-generation sequencing. We initially analyzed the TCRβ chain gene repertoire of $CD4^+$ CTLs from 4 untreated patients with active, biopsy-proved IgG_4-RD with distinct clinical features. We found that $CD4^+$ CTLs were oligoclonally expanded, typically with a single dominant clone representing 15% to 50% of all the in-frame V-D-J rearrangements detected (Fig 3, *A* and *B*). Several minor clones were also seen in each patient. In contrast, the repertoire of $CD4^+$ T cells from 4 healthy control subjects analyzed was highly diverse, and no dominant clones were observed in these subjects (Fig 3, *A*, and see Fig E7, *A*, in this article's Online Repository at www.jacionline.org). Vβ-Jβ gene segment use of the most expanded clones was not identical across patients with IgG_4-RD, and there were no clones with shared CDR3 sequences across subjects; diseased patients have diverse MHC class II alleles (data not shown). The TCR Vβ gene use in a subset of expanded $CD4^+$ CTL clones, as

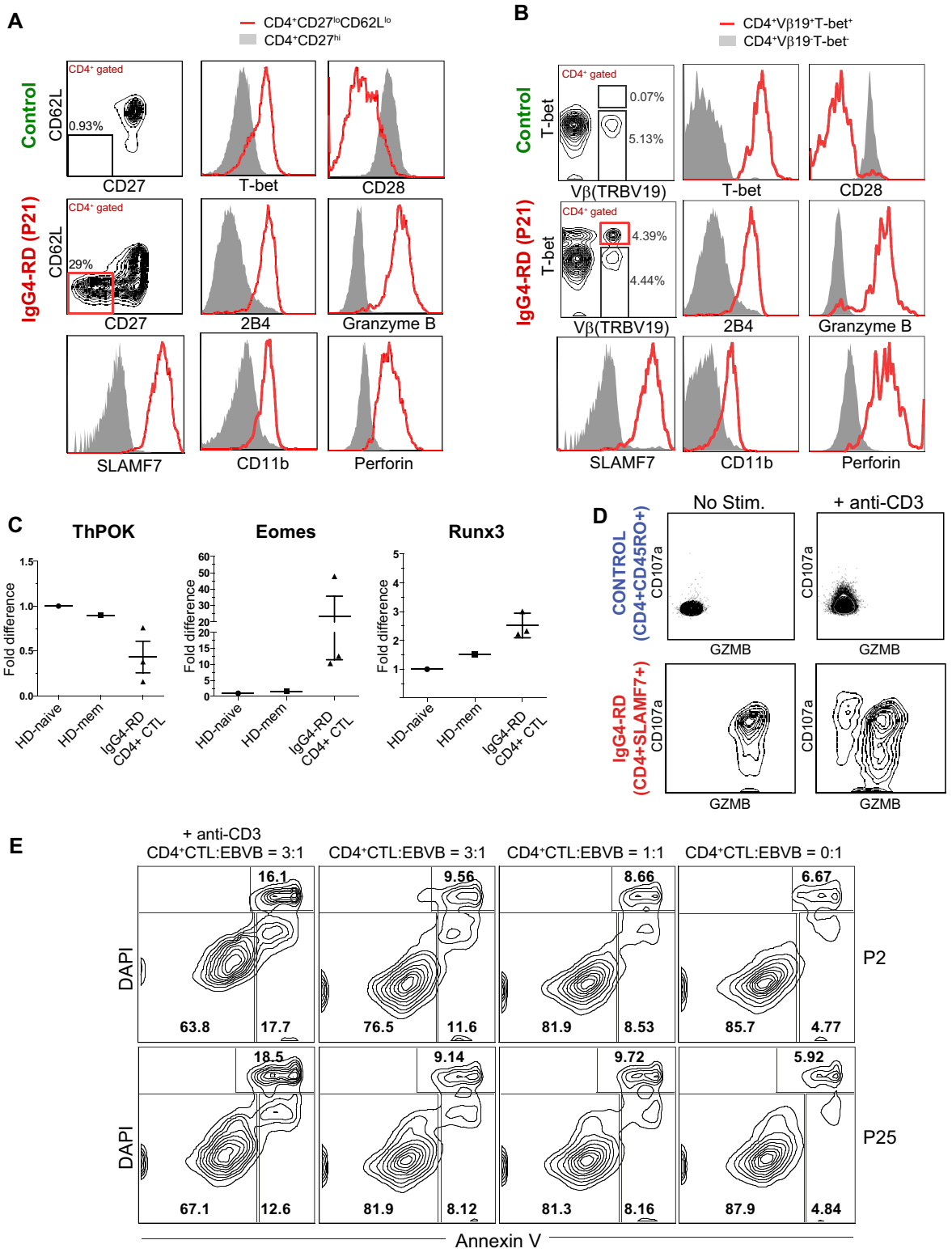


FIG 2. Expanded T_{EM} cells in patients with IgG_4-RD exhibit a functional cytolytic profile. **A** and **B,** Key hits from the gene expression analysis from Fig 1 were validated by using flow cytometry in T_{EM} cells (Fig 2, *A*) and TCR Vβ–specific antibodies (Fig 2, *B*). **C,** ThPOK and Runx3 levels in $CD4^+SLAMF7^+$ CTLs from patients with IgG_4-RD and $CD4^+CD45RO^+$ T cells from healthy control subjects. *Error bars* show SEMs. *P* values are based on the Mann-Whitney test. **D,** Granzyme B and CD107a staining on $CD4^+$ CTLs from a patient with IgG_4-RD before and after stimulation with anti-CD3. **E,** Cytotoxicity of *in vitro*–expanded $CD4^+$ CTLs derived from 2 patients (patients P2 and P25) against an allogeneic EBV-transformed B-cell target cell line measured after 12 hours of coculture with or without anti-CD3 (10 μg/mL) at varying $CD4^+$ CTL/target ratios. Data are representative of 2 separate experiments done on 4 patients. *DAPI*, 4′-6-Diamidino-2-phenylindole dihydrochloride.

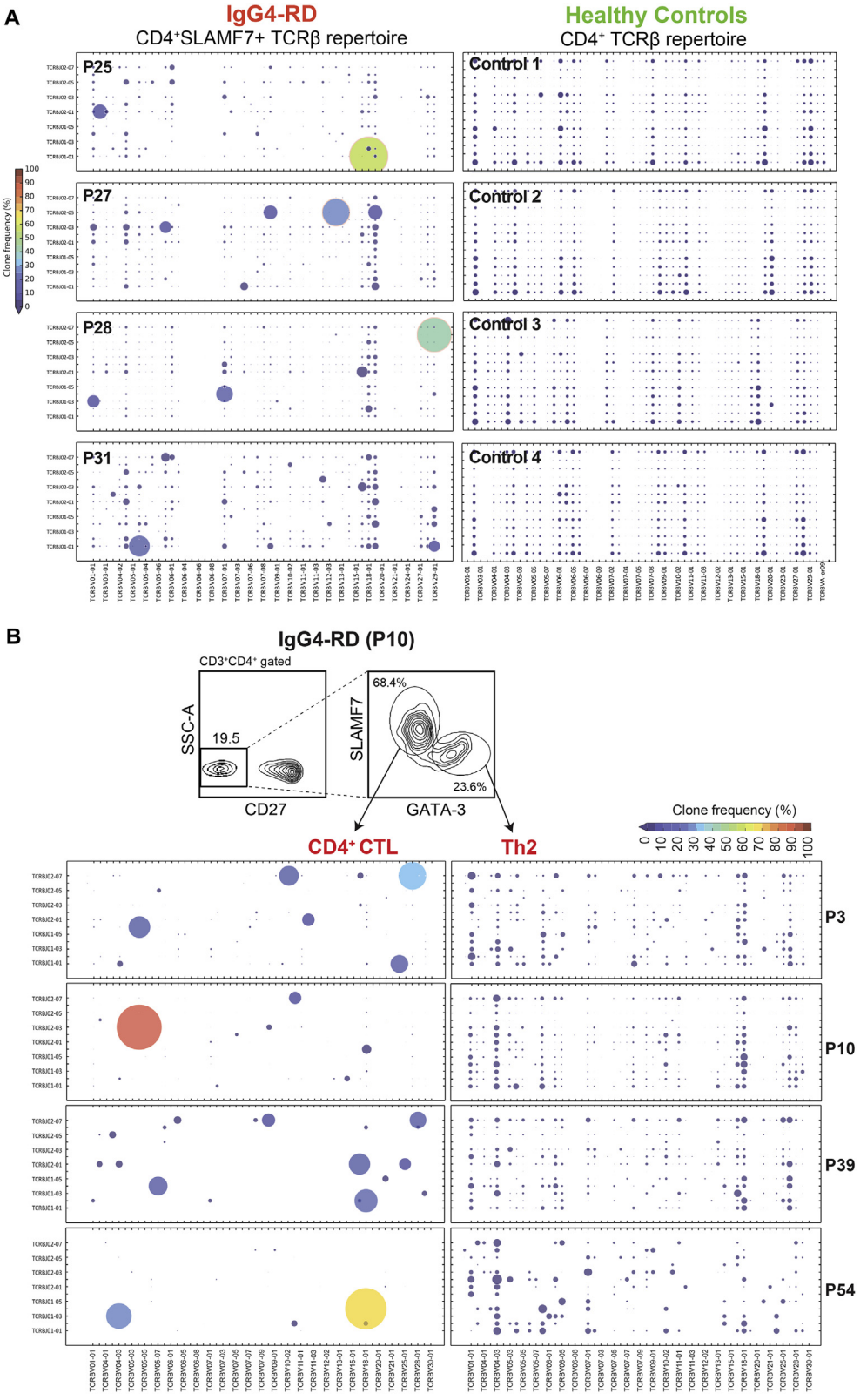


FIG 3. The TCR Vβ repertoire of expanded T_{EM} cells in patients with IgG_4-RD. **A,** TCRβ repertoire of the expanded circulating T_{EM} cell subset in 4 patients with IgG_4-RD (patients with P31, P28, P27, and P25) and total $CD4^+$ T cells from 4 healthy control subjects represented as bubble charts, where the size and color corresponds to the frequency of the observed Vβ-Jβ rearrangements. **B,** TCRβ repertoire of expanded circulating $CD4^+GATA3^+$ T_H2 cells in 4 patients with IgG_4-RD with an atopic history (patients P3, P10, P39, and P54) contrasted with expanded $CD4^+SLAMF7^+$ CTLs from the same subjects. See the legend for Fig 3, *A*, for details.

determined by using next-generation sequencing, was validated with TCR Vβ–specific antibodies in all 3 subjects for whom Vβ-specific antibodies could be obtained (see Fig E7, *B* and *C*).

In 4 atopic patients with IgG_4-RD (patients P3, P10, P39. and P54), in whom circulating $CD4^+GATA3^+$ memory T_H2 cells and $CD4^+SLAMF7^+$ CTLs were expanded, we performed massively parallel sequencing of the TCR Vβ chain to investigate the clonal diversity of these $CD4^+$ T-cell subsets. $CD4^+SLAMF7^+$ CTLs were highly oligoclonal, with 1 or a few expanded clones representing up to approximately 80% of the productive sequencing reads (Fig 3, *B*). In contrast, when analyzing simultaneously expanded $GATA3^+CD4^+$ T cells, even the most expanded clones represented less than 2% of the sequencing reads in all 4 subjects. These data strongly imply that $CD4^+SLAMF7^+$ CTLs have expanded in response to a specific causal antigen and might thus have a direct role in disease pathogenesis. In contrast, the repertoire of T_H2 phenotype cells might reflect the accumulated T-cell memory acquired over time against a wide range of environmental allergens.

$CD4^+SLAMF7^+$ CTLs can be identified in both the circulation and fibrotic lesions

$CD4^+SLAMF7^+$ CTL numbers were increased in the peripheral blood of 101 patients with IgG_4-RD compared with those in healthy control subjects ($P < .01$; Fig 4, *A*, and see Fig E8 in this article's Online Repository at www.jacionline.org). Unlike circulating $GATA3^+$ T_H2 memory cells, $CD4^+SLAMF7^+$ CTLs were abundant in both patients with and without atopy (see Fig E9 in this article's Online Repository at www.jacionline.org). A segment of diseased aorta obtained at autopsy from a previously described patient (patient P51) who succumbed to IgG_4-RD showed the presence of $CD4^+SLAMF7^+$ cells in the vessel wall by using flow cytometric analysis (Fig 4, *B*).[38] Similarly, $CD4^+SLAMF7^+$ cells were also detected in biopsy specimens from the involved nasal septum from a patient (patient P43) with IgG_4-related midline destructive lesions (Fig 5, *B*).[39]

We quantitatively analyzed tissue sections from the affected organs of 10 patients with IgG_4-RD for whom well-preserved biopsy specimens were available for the presence of $GATA3^+$ T_H2 cells and $SLAMF7^+CD4^+$ CTLs. The organs studied included submandibular glands (2 patients), lymph nodes (3 patients), and nasal palate/septum, retroperitoneal masses, kidney, and lung (1 patient each). In these affected organs infiltrating $CD4^+SLAMF7^+$ CTLs vastly outnumbered the sparse $CD4^+GATA3^+$ T_H2 T cells in all the patients with IgG_4-RD studied, including both atopic and nonatopic subjects (Fig 4, *C* and *D*). These data suggest that T_H2 cells are unlikely to be the primary drivers of pathogenicity in patients with IgG_4-RD, whereas $CD4^+$ CTLs appear, by all criteria examined, to be intimately linked to the pathogenesis of this disease. Abundance of $CD4^+SLAMF7^+$ CTLs in IgG_4-RD lesions was also confirmed in the affected organs of 20 patients with IgG_4-RD (see Fig E10, *A*, in this article's Online Repository at www.jacionline.org). In 1 patient with IgG_4-RD (patient P25), the expanded $V\beta17^+$ T_{EM} cell clone that was dominant in the circulation (Fig 2, *A*) was also found to be abundant in an inflamed tissue site (see Fig E10, *B*). $CD4^+SLAMF7^+$ CTLs also expressed granzyme A in IgG_4-RD lesions (see Fig E11 in this article's Online Repository at www.jacionline.org). These data suggest that expanded $CD4^+$ CTLs are abundant in involved tissues and might be directly involved in the pathogenesis of IgG_4-RD.

$CD4^+SLAMF7^+$ CTLs secrete the profibrotic cytokines IFN-γ, IL-1β, and TGF-β1

PBMCs were briefly restimulated with phorbol 12-myristate 13-acetate and ionomycin to mimic TCR signaling, followed by intracellular staining for T-bet, IFN-γ, and IL-4, to understand the functional behavior of the disease-related $CD4^+$ CTLs. Because T-bet is a lineage-determining transcription factor exclusively expressed in all the clonally expanded $CD4^+$ CTLs in patients with IgG_4-RD (Fig 2, *A* and *B*), we identified restimulated $CD4^+$ CTLs among total $CD4^+$ lymphocytes using T-bet staining. We did not identify any $T\text{-}bet^+$ cells that lacked the expression of perforin or granzyme B and that could therefore represent *bona fide* T_H1 cells in these patients (Fig 2, *A* and *B*). Restimulated $CD4^+$ CTLs cells from all patients with IgG_4-RD made large amounts of IFN-γ but no IL-4 (Fig 5, *A*). Clonally expanded $CD4^+$ CTLs identified by using specific TCR Vβ antibody staining consistently expressed IFN-γ but not IL-4 on restimulation (see Fig E12 in this article's Online Repository at www.jacionline.org).

IL-1β was the most prominent cytokine at the mRNA level in the expanded T_{EM} cell population. We also analyzed IL-1β at the protein level along with other cytokines more typically seen in effector T cells. Human $CD4^+$ T cells are known to express pro–IL-1β, which is processed and secreted as bioactive IL-1β on LPS stimulation.[40] We sought to determine whether $CD4^+SLAMF7^+$ cells release the processed form of IL-1β after stimulation. On *in vitro* restimulation with phorbol 12-myristate 13-acetate and ionomycin, IL-1β–producing cells were more abundant in flow-sorted $CD4^+CD45RO^+$ T cells from patients with IgG_4-RD, as detected by using ELISpot analysis, compared with $CD4^+CD45RO^+$ T cells from healthy control subjects (Fig 5, *B*). Flow-sorted $CD4^+$ CTLs cells contained more IL-1β–producing cells than naive $CD4^+CD45RA^+$ T cells from 4 patients with IgG_4-RD (Fig 5, *C*). These cells could be expanded *in vitro* and maintained in IL-2 with intermittent TCR stimulation without a loss of phenotype (see Fig E4). The expanded $CD4^+$ CTLs retained their SLAMF7 expression and cytotoxic markers and were found to secrete the processed form (17 kDa) of IL-1β on restimulation with either anti-CD3 or LPS, as determined by mean of Western blot analysis of culture supernatants (Fig 5, *D*). The amount of IL-1β secreted was comparable with the amount secreted by myeloid cells exposed to LPS.

Given the role of TGF-β1 in many fibrotic diseases, we examined the ability of $CD4^+$ CTLs to make TGF-β1 *ex vivo*, as well as at sites of disease. On *in vitro* stimulation, flow-sorted $CD4^+$ CTLs secreted large amounts of TGF-β1 compared with naive $CD4^+$ cells from the same patients (Fig 5, *E*).

Multicolor immunofluorescence staining of the affected organs of 22 patients with IgG_4-RD showed high IL-1β expression in a large proportion of $CD4^+SLAMF7^+$ cells (Fig 6, *A*, and see Fig E13 in this article's Online Repository at www.jacionline.org). Furthermore, a large number of $CD4^+TGF\text{-}\beta1^+$ T cells were detected in biopsy specimens at the sites of IgG_4-RD lesions (Fig 6, *B*, and see Fig E14 in this article's Online Repository at www.jacionline.org). These data suggest that $CD4^+$ CTLs have a profibrotic potential and might be drivers of fibrosis in IgG_4-RD lesions.

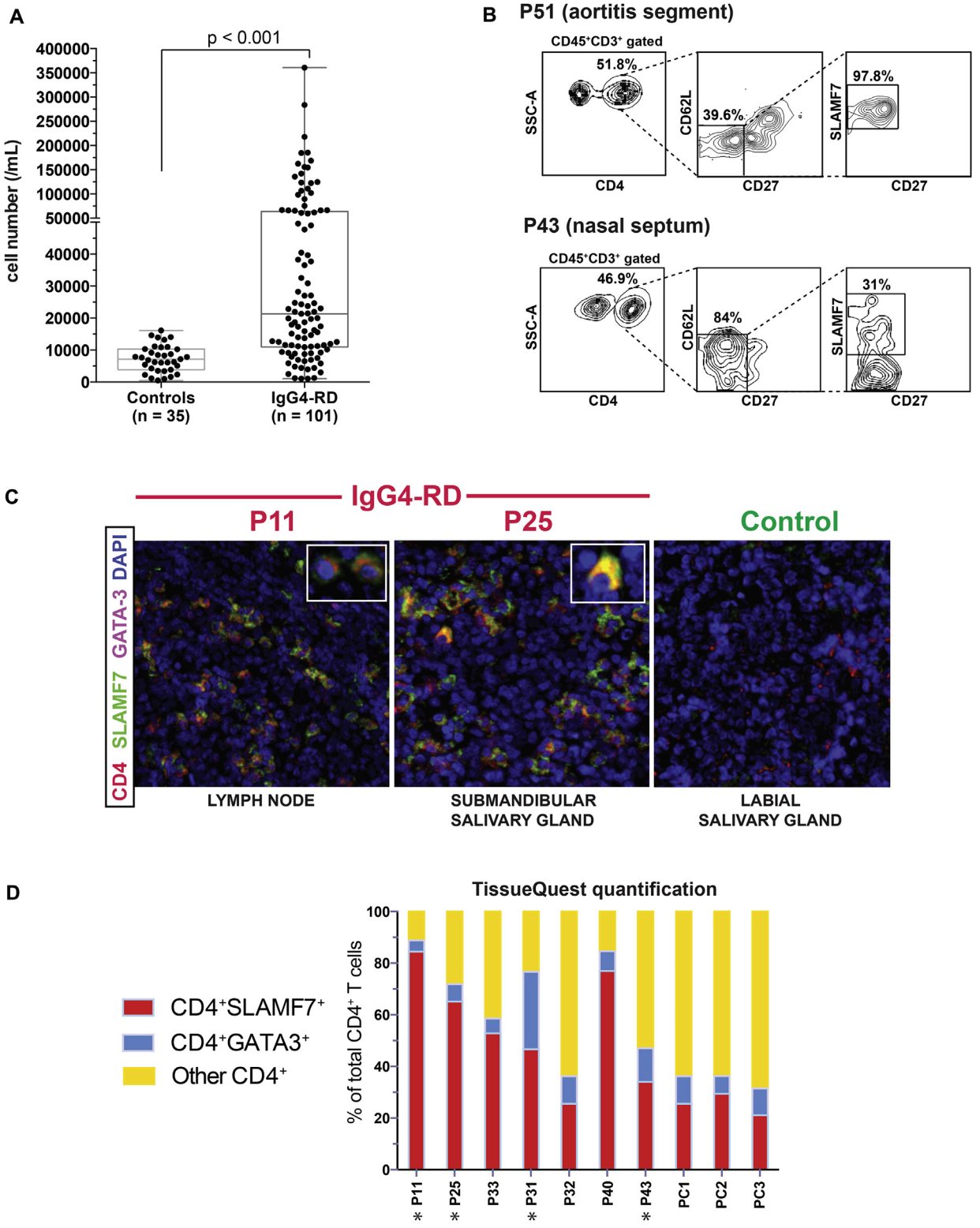


FIG 4. Expansion of $CD4^+SLAMF7^+$ CTLs in tissue lesions of patients with IgG_4-RD. **A,** Expansion of $CD4^+SLAMF7^+$ CTLs in 101 patients with IgG_4-RD. **B,** $CD4^+CD62L^{lo}CD27^{lo}SLAMF7^+$ CTLs in the aortic wall of a patient with IgG_4-related aortitis (patient P51) and the involved nasal septum of a patient with IgG_4-RD (patient P43). **C,** Immunofluorescence staining of $CD4^+SLAMF7^+$ CTLs and $CD4^+GATA3^+$ T_H2 cells in the affected tissues of patients with IgG_4-RD (lymph node biopsy specimen from patient P11 and salivary gland biopsy specimen from patient P25). CD4 *(red)*, 4′-6-diamidino-2-phenylindole dihydrochloride (*DAPI*; *blue*), GATA3 *(magenta)*, and SLAMF7 *(green)* staining is shown. **D,** Quantification of $CD4^+SLAMF7^+$, $CD4^+GATA3^+$, and $CD4^+SLAMF7^-GATA3^-$ cells in tissue biopsy specimens from 10 patients with IgG_4-RD (atopic patients are marked with *asterisks*).

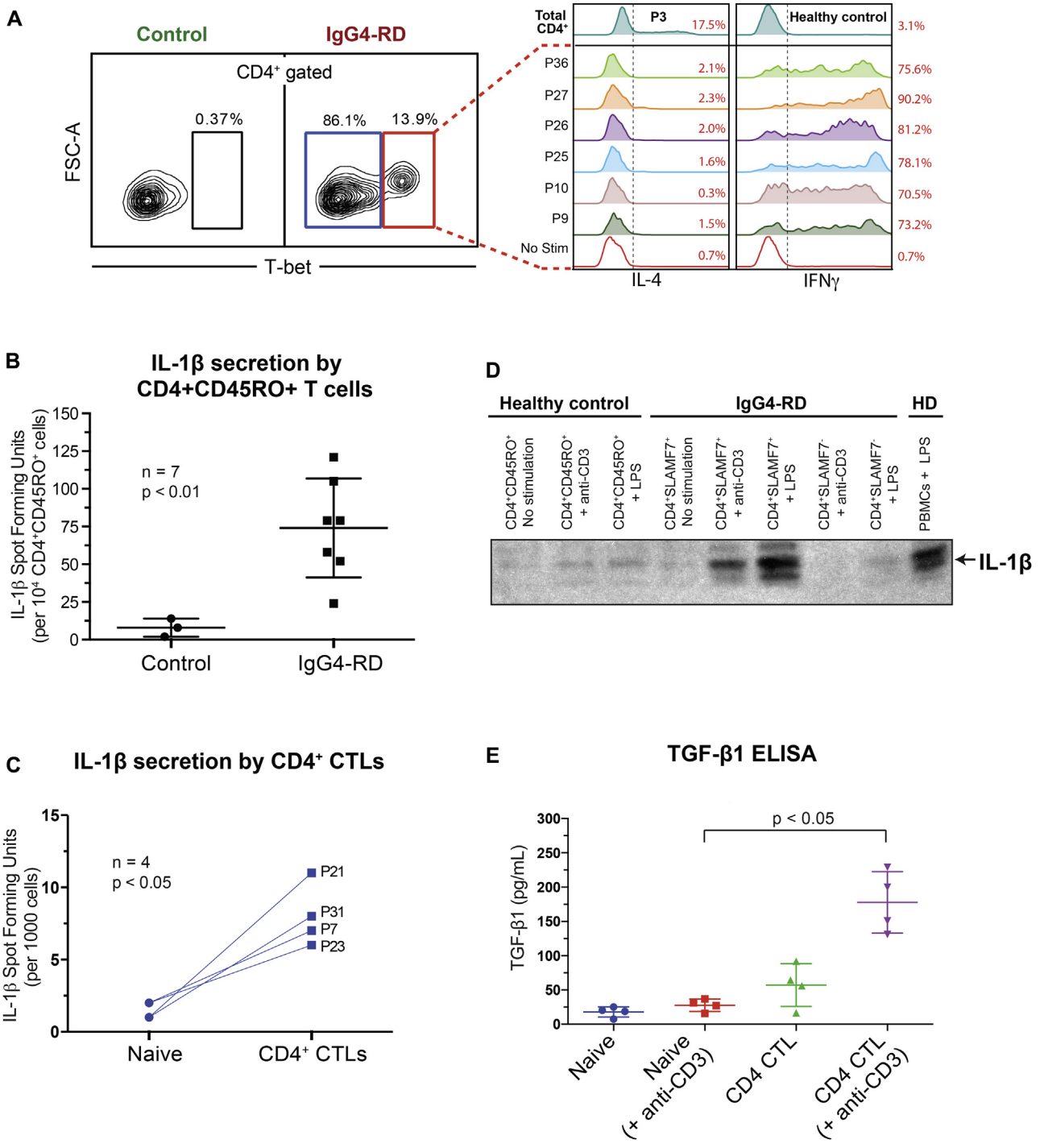


FIG 5. Disease-associated $CD4^+$ CTLs secrete IFN-γ, IL-1β, and TGF-β1 on *in vitro* restimulation. **A,** Intracellular staining for IFN-γ and IL-4 in restimulated $CD4^+$ CTLs from 7 patients with IgG_4-RD. The empty histogram *(red)* depicts an unstimulated control subject. *FSC,* Forward scatter. **B** and **C,** ELISpot detection of the frequency of IL-1β producers among restimulated $CD4^+CD45RO^+$ T cells from 7 patients with IgG_4-RD compared with healthy donors (*error bars* show SEMs, unpaired *t* test; Fig 5, *B*) and $CD4^+$ CTLs from 4 patients with IgG_4-RD compared with naive $CD4^+CD45RA^+$ T cells from the same subjects ($P < .05$, paired *t* test; Fig 5, *C*). **D,** Western blot detection of IL-1β from culture supernatants of *in vitro*–expanded T cells maintained in IL-2 for 2 weeks (10 ng/mL). Supernatants from $CD4^+CD45RO^+$ T cells from a healthy donor and $CD4^+CD45RO^+SLAMF7^+$ or $CD4^+CD45RO^+SLAMF7^-$ T cells from a patient with IgG_4-RD were used without any stimulation with 5 μg/mL LPS or 3 μg/mL anti-CD3. LPS-stimulated PBMCs from a healthy donor *(HD)* were used as a positive control. **E,** Detection of TGF-β1 production among naive $CD4^+$ cells and $CD4^+SLAMF7^+$ CTLs from 4 patients with IgG_4-RD by using ELISA with or without *in vitro* restimulation (with 3 μg/mL anti-CD3). *Error bars* show SEMs. *P* values are based on the Mann-Whitney test.

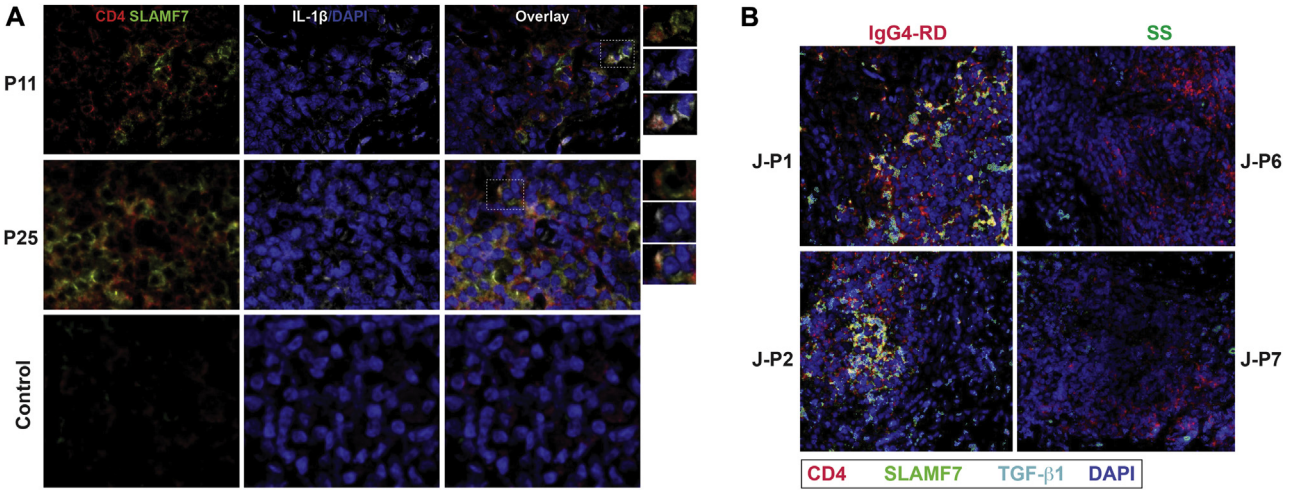


FIG 6. Expansion of IL-1β– and TGF-β1–secreting $CD4^+$ CTLs in IgG_4-RD lesions. **A,** Immunofluorescence staining of IL-1β–producing $CD4^+SLAMF7^+$ cells in the tissue of 2 patients with IgG_4-RD (lymph node biopsy specimen from patient P11 and salivary gland biopsy specimen from patient P25) and a healthy control subject (labial salivary gland biopsy specimen). CD4 *(red)*, SLAMF7 *(green)*, 4′-6-diamidino-2-phenylindole dihydrochloride (DAPI; *blue*), and IL-1β *(white)* staining is shown. **B,** Immunofluorescence staining of TGF-β1–producing $CD4^+SLAMF7^+$ cells in the tissues of 2 patients with IgG_4-related dacryoadenitis and sialadenitis and 2 patients with Sjögren syndrome (*SS*; submandibular salivary gland biopsy specimens). CD4 *(red)*, granzyme A *(green)* DAPI *(blue)*, and IL-1β *(cyan)* staining is shown.

Circulating $CD4^+SLAMF7^+$ CTL numbers diminish in patients with IgG_4-RD after rituximab therapy

Therapeutic B-cell depletion with rituximab (an anti-CD20 mAb) generally results in clinical improvement in patients with IgG_4-RD.[41,42] $CD19^+$ B-cell numbers decrease dramatically after rituximab therapy, followed by a clinically apparent reduction in disease activity, as measured by using the IgG_4-RD Responder Index.[43] Interestingly, a significant decrease in percentages and numbers of $CD4^+SLAMF7^+$ CTLs was also observed up to 12 months after rituximab treatment, whereas the number of naive $CD4^+CD45RA^+$ T cells remained stable (Fig 7, *A* and *B*).

Rituximab therapy had minimal or no effect on the frequency and number of $CD4^+GATA3^+$ T_H2 phenotype cells or $CD4^+CD25^+Foxp3^+$ regulatory T cells in peripheral blood (Fig 7, *C* and *D*). $CD4^+SLAMF7^+$ CTL numbers decreased despite the fact that these cells do not express any detectable CD20 on their cell surfaces (see Fig E15 in this article's Online Repository at www.jacionline.org). In one serially monitored subject, for whom a TCR Vβ–specific antibody was available, rituximab treatment induced a decrease in the $V\beta17^+$ CTL clone, as well as a decrease in total $CD4^+SLAMF7^+$ CTL numbers (Fig 7, *E*). A positive clinical response to rituximab therapy was accompanied by a greater than 50% reduction in circulating $CD4^+SLAMF7^+$ CTL numbers (Fig 7, *F*). These data provide additional circumstantial evidence for a pathogenic role for IL-1β–secreting $CD4^+$ CTLs in patients with IgG_4-RD.

DISCUSSION

One of the challenges in human immunology is the difficulty in advancing from correlation to causation. Our studies reveal that a poorly studied human $CD4^+$ T-cell population that secretes profibrotic cytokines is expanded in patients with IgG_4-RD. The demonstration of the clonal expansion of these T cells by means of next-generation sequencing, their localization and *in situ* reactivation at sites of disease, and their decrease after successful therapy provide strong evidence for a likely causal role for IL-1β–, IFN-γ–, and TGF-β1–secreting $CD4^+$ cytotoxic T cells in patients with IgG_4-RD and likely other fibrotic inflammatory disorders. Such an approach, determining which lymphocytes are clonally expanded and infiltrate tissue sites of disease, might serve as a template for implicating specific adaptive immune cells in disease processes.

This study illustrates several novel and clinically relevant findings. Oligoclonal expansions of circulating $CD4^+SLAMF7^+$ CTLs are seen in patients with IgG_4-RD, especially during active disease. These T-cell clones are unusual in terms of their ability to make IL-1β, TGF-β1, and IFN-γ; IL-1β is a cytokine typically thought to be produced by nonlymphoid cells.[44] These expanded T cells were also found in affected tissues, providing strong evidence for their potential role in disease pathogenesis. The production of large amounts of IL-1β by these T cells after brief restimulation and the expression of preformed cytotoxic mediators suggest that the $CD4^+SLAMF7^+$ CTL population represents an unusual and not easily categorized subset of human $CD4^+$ effector T cells that potentially drives the disease process, perhaps in collaboration with other T cells. The secretion of processed IL-1β suggests that inflammasome activation occurs in activated $CD4^+$ CTLs. The mechanism of TGF-β1 induction in $CD4^+$ CTLs and the presumed processing of secreted TGF-β1 in diseased tissues remains to be investigated.

Fibrosis is an essential feature of the histopathology of IgG_4-RD,[45] but the cause of the fibrosis in patients with this disease has not been clear. IgG_4 antibodies are generally considered noninflammatory because they do not efficiently engage activating Fc receptors or complement and might be functionally monovalent *in vivo*.[46] We have observed active disease in a number of patients with relatively low levels of plasma IgG_4 but a clear expansion of the $CD4^+SLAMF7^+$ CTL population. Therefore the contribution of IgG_4 antibodies to disease pathogenesis is unclear.

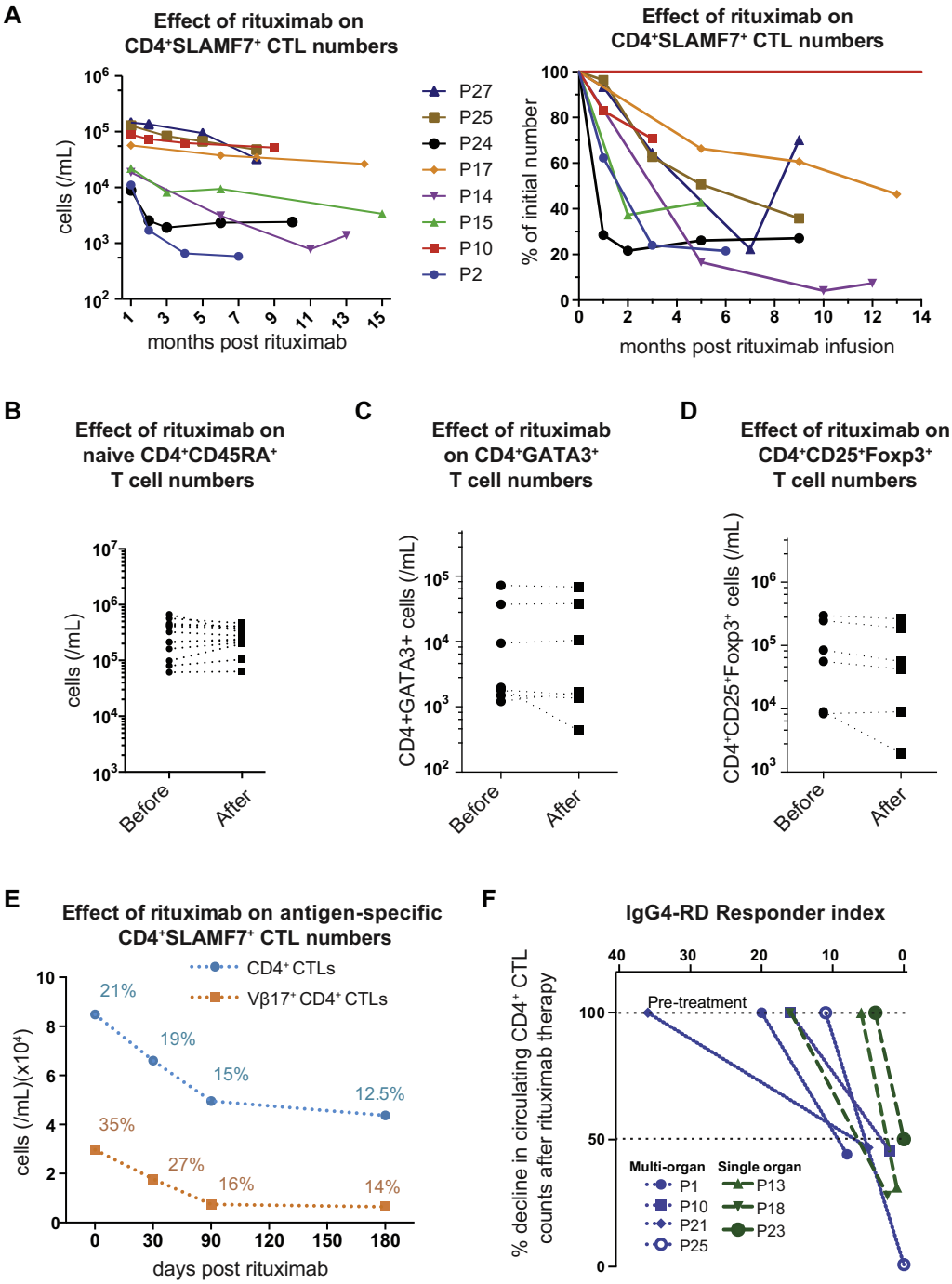


FIG 7. Rituximab-mediated depletion of $CD4^+$ CTLs. **A,** Decrease in $CD4^+SLAMF7^+$ CTL numbers (n = 8 subjects) over 6 to 14 months after rituximab infusion shown as a change in cell counts and proportion. **B,** Effect of rituximab on $CD4^+CD45RA^+$ naive T-cell counts in peripheral blood of patients with IgG_4-RD. **C** and **D,** Effect of rituximab on $CD4^+GATA3^+$ T_H2 cells and $CD4^+CD25^+Foxp3^+$ cells in peripheral blood of patients with IgG_4-RD 90 to 120 days after rituximab therapy. **E,** Decrease in the number and proportion of an expanded $CD4^+$ CTL clone tracked by using a TCR Vβ–specific antibody after rituximab therapy in a patient with IgG4-RD (patient P25). **F,** Decrease in circulating $CD4^+$ CTL numbers at days 70 to 95 after rituximab therapy (normalized to pretreatment levels) is plotted against the IgG_4-RD Responder Index, a clinical measure of disease activity.

It is possible that the IgG_4 response seen in patients with this disease represents an exaggerated but ineffectual attempt to sequester antigens and dampen inflammation.

Our observations show that clonally expanded $CD4^+$ CTLs that express granzyme B, perforin, IFN-γ, IL-1β, and TGF-β1 are prominent in patients with this disease, and a number of prior

observations suggest that they might induce the fibrotic pathology seen in patients with IgG_4-RD. Transient expression of IL-1β alone in the rat lung has been shown to result in tissue damage and progressive fibrosis.[17] Transgenic overexpression of IL-1β in the murine pancreas results in fibrotic pancreatitis.[18] IL-1 receptor 1/MyD88 signaling and the inflammasome are essential drivers of the fibrotic process in the widely studied murine model of pulmonary fibrosis induced by bleomycin.[16] IFN-γ has been shown to contribute to fibrosis in a murine thyroiditis model.[47] Indeed, IL-1β–induced fibrosis in mice has been shown to be dependent on IL-17A and IFN-γ. These $CD4^+$ CTLs observed in patients with IgG_4-RD represent an abundant source of IL-1β and TGF-β1 in the tissue lesions of patients with IgG_4-RD, thereby potentially driving fibrosis.

In addition to our studies on IgG_4-RD, studies on smaller numbers of subjects with systemic sclerosis suggest that $CD4^+$T-bet$^+$SLAMF7$^+$ CTLs contribute to the pathogenesis of a broader range of fibrotic inflammatory diseases (see Fig E16 in this article's Online Repository at www.jacionline.org). The abundance of these cells in patients with systemic sclerosis, for instance, is similar to that seen in patients with IgG_4-RD. $CD4^+CD28^{lo}$ cells, which have been shown to express cytotoxic mediators and IFN-γ in some studies, have previously been identified in patients with idiopathic pulmonary fibrosis, severe rheumatoid arthritis, multiple sclerosis, and granulomatosis with polyangiitis (formerly Wegener granulomatosis)[48-50] and a small proportion of healthy elderly subjects. The $CD4^+SLAMF7^+$ CTLs we have identified in patients with IgG_4-RD also express reduced levels of CD28 and might be related to these previously described $CD4^+CD28^{lo}$ cells. A survey of SLAM family protein expression in patients with systemic lupus erythematosus revealed higher levels of SLAMF7 in some B and T cells, but the cell phenotypes were not characterized further.[51]

Many types of fibrosis, including murine models of schistosomiasis and bleomycin-induced pulmonary fibrosis, have been linked to T_H2 cells and T_H2 cytokines.[19] Although T_H2 cells have been implicated in patients with IgG_4-RD in some studies,[7-9] we have recently demonstrated that T_H2 cell expansions are highly correlated with the allergic history of patients. We have not seen a consistent expansion of T_H2 effector cells in patients with active IgG_4-RD. Instead, we find that patients with IgG_4-RD with chronic allergies in addition to fibrotic tumescent lesions have an expansion of both T_H2 cells and IL-1β–producing $CD4^+$ CTLs, and clonal expansions of T_H2 cells are not seen, even in subjects with concomitant allergic disease. $CD4^+$ CTLs in patients with IgG_4-RD synthesize IL-1β and TGF-β1 in affected fibrotic tissues, suggesting that fibrotic disease mechanisms that have been elucidated downstream of IL-1β[30] and TGF-β1[3] are likely of importance in IgG_4-RD.

We have recently demonstrated marked expansions of $IgG4^+$ plasmablasts in patients with active IgG_4-RD.[52] Because these plasmablasts express high levels of MHC class II molecules, are depleted by rituximab, and are also present in disease lesions, it is possible that they play an important role in reactivation of the $CD4^+$ CTLs and induce them to either make cytokines, including IL-1β and TGF-β1, or kill parenchymal cells.

The selective decrease in $CD4^+$ CTL numbers, including the expanded clones after rituximab-mediated B-cell depletion, might have broad relevance. These observations imply that in human subjects, as in rodents, B cells play an important role in the maintenance of T_{EM} $CD4^+$ cells, including disease-associated rogue T-cell clones.[53,54] These findings might explain why rituximab is effective in patients with diseases such as relapsing-remitting multiple sclerosis, in which end-organ damage is primarily mediated by autoreactive T cells. B cells that have the unique ability to bind specific autoantigens can act as potent antigen-presenting cells at low antigen concentrations[55] and might provide efficient access to T-cell epitopes. Thus it is possible that in patients with T cell–mediated autoimmune disorders that are responsive to rituximab therapy, the $CD4^+$ T_{EM} cell response is maintained by B cells. Alternatively, pathogenic T cells might be dependent on B–cell derived growth factors.[53] These possibilities are not mutually exclusive.

The SLAM family is a subset of the immunoglobulin superfamily of receptors. Members of the SLAM family can be involved in both homotypic and heterotypic interactions.[56,57] Given the presence of immune receptor tyrosine-based switch motifs in its cytoplasmic tail, SLAMF7 can lead to activating or inhibitory signaling within the cell, depending on its association with a SLAM-associated protein family adaptor called EAT2. Both plasmablasts and $CD4^+$ CTLs in diseased tissue express SLAMF7, and it is unclear at this time whether SLAMF7 in $CD4^+$ CTLs participates in homotypic or heterotypic interactions or whether it transduces activating or inhibitory signals in these cells.

From a therapeutic standpoint, depleting SLAMF7-expressing cells, as well as neutralizing IL-1β, might represent rational strategies in a range of immune-mediated conditions associated with severe tissue damage and fibrosis. A few biologic agents that target SLAMF7 or IL-1β are already in clinical use or in advanced stages of drug development. A humanized mAb directed against the human SLAMF7, elotuzumab, has shown promise in patients with advanced multiple myeloma.[58] Anakinra, a nonglycosylated recombinant form of the naturally occurring IL-1 receptor antagonist that blocks inflammasome-dependent IL-1β signaling, has been successfully used in type 2 diabetes, asbestosis, and other conditions.[59] Canakinumab is an mAb that binds to and antagonizes IL-1β and is being studied in a number of clinical trials.[60]

In summary, our studies suggest that $CD4^+$ CTLs with a unique and hitherto undescribed phenotype expand clonally in the circulation and tissue sites and probably mediate the pathologic changes seen in patients with IgG_4-RD. These cells elaborate a unique combination of cytokines, some of which are known to contribute to fibrosis in animal models, and the numbers of these cells correlate well with clinical disease activity. Furthermore, therapeutic improvement in patients with IgG_4-RD mediated by B-cell depletion is linked to a specific reduction in numbers of these $CD4^+$ CTLs and not of naive T cells, regulatory T cells, or memory follicular T helper cells. Examining subjects with newly diagnosed, untreated, and active disease has allowed the identification and characterization of clonally expanded effector T cells linked to disease and to the observation of their attenuation by rituximab. These studies suggest a mechanism by which rituximab mediates clinical improvement in inflammatory disorders that are primarily linked to T cells. Based on our studies, we believe that B-cell depletion will also likely prove effective in other immune-mediated disorders involving pathogenic effector T-cell subsets that depend on B cells for antigen presentation or maintenance.

Key messages

- **$CD4^+$ T effector memory cells with cytolytic and myeloid features are expanded in patients with IgG_4-RD.**
- **$CD4^+SLAMF7^+$ CTLs are clonally expanded, whereas $CD4^+GATA3^+$ T_H2 memory cells in atopic patients with IgG_4-RD are clonally diverse. $GATA3^+$ T_H2 cells represent a minor proportion of $CD4^+$ cells in affected tissues.**
- **In patients with IgG_4-RD, $CD4^+SLAMF7^+$ CTLs infiltrate the diseased tissues and secrete the profibrotic cytokines IL-1β and TGF-β1.**
- **The decrease in $CD4^+SLAMF7^+$ CTL numbers on rituximab therapy is associated with clinical remission in patients with IgG_4-RD.**

REFERENCES

1. Stone JH, Zen Y, Deshpande V. IgG4-related disease. N Engl J Med 2012;366:539-51.
2. Mahajan VS, Mattoo H, Deshpande V, Pillai SS, Stone JH. IgG4-related disease. Annu Rev Pathol 2014;9:315-47.
3. Kamisawa T, Zen Y, Pillai S, Stone JH. IgG4-related disease. Lancet 2015;385:1460-71.
4. Bindon CI, Hale G, Bruggemann M, Waldmann H. Human monoclonal IgG isotypes differ in complement activating function at the level of C4 as well as C1q. J Exp Med 1988;168:127-42.
5. Bruhns P, Iannascoli B, England P, Mancardi DA, Fernandez N, Jorieux S, et al. Specificity and affinity of human Fcgamma receptors and their polymorphic variants for human IgG subclasses. Blood 2009;113:3716-25.
6. Aoki S, Nakazawa T, Ohara H, Sano H, Nakao H, Joh T, et al. Immunohistochemical study of autoimmune pancreatitis using anti-IgG4 antibody and patients' sera. Histopathology 2005;47:147-58.
7. Tanaka A, Moriyama M, Nakashima H, Miyake K, Hayashida JN, Maehara T, et al. Th2 and regulatory immune reactions contribute to IgG4 production and the initiation of Mikulicz disease. Arthritis Rheum 2012;64:254-63.
8. Kanari H, Kagami S, Kashiwakuma D, Oya Y, Furuta S, Ikeda K, et al. Role of Th2 cells in IgG4-related lacrimal gland enlargement. Int Arch Allergy Immunol 2010;152(suppl 1):47-53.
9. Zen Y, Fujii T, Harada K, Kawano M, Yamada K, Takahira M, et al. Th2 and regulatory immune reactions are increased in immunoglobin G4-related sclerosing pancreatitis and cholangitis. Hepatology 2007;45:1538-46.
10. Okazaki K, Uchida K, Ohana M, Nakase H, Uose S, Inai M, et al. Autoimmune-related pancreatitis is associated with autoantibodies and a Th1/Th2-type cellular immune response. Gastroenterology 2000;118:573-81.
11. Johnson S, Eller M, Teigler JE, Maloveste SM, Schultz BT, Soghoian DZ, et al. Cooperativity of HIV-specific cytolytic CD4 T cells and CD8 T cells in control of HIV viremia. J Virol 2015;89:7494-505.
12. Della Torre E, Mattoo H, Mahajan VS, Carruthers M, Pillai S, Stone JH. Prevalence of atopy, eosinophilia, and IgE elevation in IgG4-related disease. Allergy 2014;69:269-72.
13. Mattoo H, Della-Torre E, Mahajan VS, Stone JH, Pillai S. Circulating Th2 memory cells in IgG4-related disease are restricted to a defined subset of subjects with atopy. Allergy 2014;69:399-402.
14. Wick G, Backovic A, Rabensteiner E, Plank N, Schwentner C, Sgonc R. The immunology of fibrosis: innate and adaptive responses. Trends Immunol 2010;31:110-9.
15. Wynn TA, Ramalingam TR. Mechanisms of fibrosis: therapeutic translation for fibrotic disease. Nat Med 2012;18:1028-40.
16. Gasse P, Mary C, Guenon I, Noulin N, Charron S, Schnyder-Candrian S, et al. IL-1R1/MyD88 signaling and the inflammasome are essential in pulmonary inflammation and fibrosis in mice. J Clin Invest 2007;117:3786-99.
17. Kolb M, Margetts PJ, Anthony DC, Pitossi F, Gauldie J. Transient expression of IL-1beta induces acute lung injury and chronic repair leading to pulmonary fibrosis. J Clin Invest 2001;107:1529-36.
18. Marrache F, Tu SP, Bhagat G, Pendyala S, Osterreicher CH, Gordon S, et al. Overexpression of interleukin-1beta in the murine pancreas results in chronic pancreatitis. Gastroenterology 2008;135:1277-87.
19. Wynn TA. Fibrotic disease and the T(H)1/T(H)2 paradigm. Nat Rev Immunol 2004;4:583-94.
20. Doucet C, Brouty-Boye D, Pottin-Clemenceau C, Canonica GW, Jasmin C, Azzarone B. Interleukin (IL) 4 and IL-13 act on human lung fibroblasts. Implication in asthma. J Clin Invest 1998;101:2129-39.
21. Sempowski GD, Beckmann MP, Derdak S, Phipps RP. Subsets of murine lung fibroblasts express membrane-bound and soluble IL-4 receptors. Role of IL-4 in enhancing fibroblast proliferation and collagen synthesis. J Immunol 1994;152:3606-14.
22. Fuschiotti P. Role of IL-13 in systemic sclerosis. Cytokine 2011;56:544-9.
23. Kolodsick JE, Toews GB, Jakubzick C, Hogaboam C, Moore TA, McKenzie A, et al. Protection from fluorescein isothiocyanate-induced fibrosis in IL-13-deficient, but not IL-4-deficient, mice results from impaired collagen synthesis by fibroblasts. J Immunol 2004;172:4068-76.
24. Lee CG, Homer RJ, Zhu Z, Lanone S, Wang X, Koteliansky V, et al. Interleukin-13 induces tissue fibrosis by selectively stimulating and activating transforming growth factor beta(1). J Exp Med 2001;194:809-21.
25. Murray LA, Argentieri RL, Farrell FX, Bracht M, Sheng H, Whitaker B, et al. Hyper-responsiveness of IPF/UIP fibroblasts: interplay between TGFbeta1, IL-13 and CCL2. Int J Biochem Cell Biol 2008;40:2174-82.
26. Oh MH, Oh SY, Yu J, Myers AC, Leonard WJ, Liu YJ, et al. IL-13 induces skin fibrosis in atopic dermatitis by thymic stromal lymphopoietin. J Immunol 2011;186:7232-42.
27. Weng HL, Liu Y, Chen JL, Huang T, Xu LJ, Godoy P, et al. The etiology of liver damage imparts cytokines transforming growth factor beta1 or interleukin-13 as driving forces in fibrogenesis. Hepatology 2009;50:230-43.
28. Wynn TA, Barron L. Macrophages: master regulators of inflammation and fibrosis. Semin Liver Dis 2010;30:245-57.
29. Deshpande V. The pathology of IgG4-related disease: critical issues and challenges. Semin Diagn Pathol 2012;29:191-6.
30. Johansson SG, Hourihane JO, Bousquet J, Bruijnzeel-Koomen C, Dreborg S, Haahtela T, et al. A revised nomenclature for allergy. An EAACI position statement from the EAACI nomenclature task force. Allergy 2001;56:813-24.
31. Larimore K, McCormick MW, Robins HS, Greenberg PD. Shaping of human germline IgH repertoires revealed by deep sequencing. J Immunol 2012;189:3221-30.
32. Robins HS, Campregher PV, Srivastava SK, Wacher A, Turtle CJ, Kahsai O, et al. Comprehensive assessment of T-cell receptor beta-chain diversity in alphabeta T cells. Blood 2009;114:4099-107.
33. De Jong R, Brouwer M, Hooibrink B, Van der Pouw-Kraan T, Miedema F, Van Lier RA. The CD27- subset of peripheral blood memory CD4+ lymphocytes contains functionally differentiated T lymphocytes that develop by persistent antigenic stimulation in vivo. Eur J Immunol 1992;22:993-9.
34. Sallusto F, Lenig D, Forster R, Lipp M, Lanzavecchia A. Two subsets of memory T lymphocytes with distinct homing potentials and effector functions. Nature 1999;401:708-12.
35. Koyabu M, Uchida K, Miyoshi H, Sakaguchi Y, Fukui T, Ikeda H, et al. Analysis of regulatory T cells and IgG4-positive plasma cells among patients of IgG4-related sclerosing cholangitis and autoimmune liver diseases. J Gastroenterol 2010;45:732-41.
36. Soghoian DZ, Streeck H. Cytolytic CD4(+) T cells in viral immunity. Expert Rev Vaccines 2010;9:1453-63.
37. Mucida D, Husain MM, Muroi S, van Wijk F, Shinnakasu R, Naoe Y, et al. Transcriptional reprogramming of mature CD4(+) helper T cells generates distinct MHC class II-restricted cytotoxic T lymphocytes. Nat Immunol 2013;14:281-9.
38. Stone JH, Khosroshahi A, Hilgenberg A, Spooner A, Isselbacher EM, Stone JR. IgG4-related systemic disease and lymphoplasmacytic aortitis. Arthritis Rheum 2009;60:3139-45.
39. Della-Torre E, Mattoo H, Mahajan VS, Deshpande V, Krause D, Song P, et al. IgG4-related midline destructive lesion. Ann Rheum Dis 2014;73:1434-6.
40. Yamashita M, Ukai-Tadenuma M, Miyamoto T, Sugaya K, Hosokawa H, Hasegawa A, et al. Essential role of GATA3 for the maintenance of type 2 helper T (Th2) cytokine production and chromatin remodeling at the Th2 cytokine gene loci. J Biol Chem 2004;279:26983-90.
41. Khosroshahi A, Carruthers MN, Deshpande V, Unizony S, Bloch DB, Stone JH. Rituximab for the treatment of IgG4-related disease: lessons from 10 consecutive patients. Medicine (Baltimore) 2012;91:57-66.
42. Khosroshahi A, Bloch DB, Deshpande V, Stone JH. Rituximab therapy leads to rapid decline of serum IgG4 levels and prompt clinical improvement in IgG4-related systemic disease. Arthritis Rheum 2010;62:1755-62.
43. Carruthers MN, Stone JH, Deshpande V, Khosroshahi A. Development of an IgG4-RD Responder Index. Int J Rheumatol 2012;2012:259408.
44. Dinarello CA. Immunological and inflammatory functions of the interleukin-1 family. Annu Rev Immunol 2009;27:519-50.
45. Deshpande V, Zen Y, Chan JK, Yi EE, Sato Y, Yoshino T, et al. Consensus statement on the pathology of IgG4-related disease. Mod Pathol 2012;25:1181-92.

46. Aalberse RC, Stapel SO, Schuurman J, Rispens T. Immunoglobulin G4: an odd antibody. Clin Exp Allergy 2009;39:469-77.
47. Chen K, Wei Y, Sharp GC, Braley-Mullen H. Balance of proliferation and cell death between thyrocytes and myofibroblasts regulates thyroid fibrosis in granulomatous experimental autoimmune thyroiditis (G-EAT). J Leukoc Biol 2005;77:166-72.
48. Martens PB, Goronzy JJ, Schaid D, Weyand CM. Expansion of unusual CD4+ T cells in severe rheumatoid arthritis. Arthritis Rheum 1997;40:1106-14.
49. Komocsi A, Lamprecht P, Csernok E, Mueller A, Holl-Ulrich K, Seitzer U, et al. Peripheral blood and granuloma CD4(+)CD28(-) T cells are a major source of interferon-gamma and tumor necrosis factor-alpha in Wegener's granulomatosis. Am J Pathol 2002;160:1717-24.
50. Gilani SR, Vuga LJ, Lindell KO, Gibson KF, Xue J, Kaminski N, et al. CD28 down-regulation on circulating CD4 T-cells is associated with poor prognoses of patients with idiopathic pulmonary fibrosis. PLoS One 2010;5:e8959.
51. Kim JR, Mathew SO, Patel RK, Pertusi RM, Mathew PA. Altered expression of signalling lymphocyte activation molecule (SLAM) family receptors CS1 (CD319) and 2B4 (CD244) in patients with systemic lupus erythematosus. Clin Exp Immunol 2010;160:348-58.
52. Mattoo H, Mahajan VS, Della-Torre E, Sekigami Y, Carruthers M, Wallace ZS, et al. De novo oligoclonal expansions of circulating plasmablasts in active and relapsing IgG4-related disease. J Allergy Clin Immunol 2014;134:679-87.
53. Barr TA, Shen P, Brown S, Lampropoulou V, Roch T, Lawrie S, et al. B cell depletion therapy ameliorates autoimmune disease through ablation of IL-6-producing B cells. J Exp Med 2012;209:1001-10.
54. Crawford A, Macleod M, Schumacher T, Corlett L, Gray D. Primary T cell expansion and differentiation in vivo requires antigen presentation by B cells. J Immunol 2006;176:3498-506.
55. Rock KL, Benacerraf B, Abbas AK. Antigen presentation by hapten-specific B lymphocytes. I. Role of surface immunoglobulin receptors. J Exp Med 1984;160:1102-13.
56. Veillette A, Guo H. CS1, a SLAM family receptor involved in immune regulation, is a therapeutic target in multiple myeloma. Crit Rev Oncol Hematol 2013;88:168-77.
57. De Calisto J, Wang N, Wang G, Yigit B, Engel P, Terhorst C. SAP-dependent and -independent regulation of innate T cell development involving SLAMF receptors. Front Immunol 2014;5:186.
58. Zonder JA, Mohrbacher AF, Singhal S, van Rhee F, Bensinger WI, Ding H, et al. A phase 1, multicenter, open-label, dose escalation study of elotuzumab in patients with advanced multiple myeloma. Blood 2012;120:552-9.
59. Menu P, Vince JE. The NLRP3 inflammasome in health and disease: the good, the bad and the ugly. Clin Exp Immunol 2011;166:1-15.
60. Chakraborty A, Tannenbaum S, Rordorf C, Lowe PJ, Floch D, Gram H, et al. Pharmacokinetic and pharmacodynamic properties of canakinumab, a human anti-interleukin-1beta monoclonal antibody. Clin Pharmacokinet 2012;51:e1-18.

Rituximab infusion of IgG4-RD patients.

This study was approved by the institutional review board and informed, written consent was obtained from all subjects referred to or presenting at the rheumatology clinic of the Massachusetts General Hospital. Twelve IgG4-RD patients with active disease were treated with two 1000 mg doses of rituximab, 15 days apart. 15 mL of peripheral blood was collected at initial presentation and each subsequent clinical visit. These patients were longitudinally followed for 9-15 months at the rheumatology clinic. Peripheral blood was collected in EDTA or ACD tubes (BD Vacutainer) and transported to the laboratory for cell isolation on the same day.

Isolation of mononuclear cells: Mononuclear cells were isolated from peripheral blood of IgG4-RD subjects and healthy controls by Ficoll-Paque Plus (GE Healthcare) density-gradient centrifugation following the manufacturer's protocol. To facilitate subsequent analysis of cells in batches, PBMCs were resuspended in fetal bovine serum containing 10% dimethyl sulfoxide and cryopreserved in vapor phase liquid nitrogen.

Immunofluorescence: Anti-human TCRVβ17-PE (clone E17.5F3.15.13, Beckman-Coulter), anti-human CD4-biotin and mouse anti-biotin Alexa fluor 647 (Life technologies), mouse anti-human CD319 (clone 162.1, Biolegend) and goat anti-mouse Alexa fluor 488 (Life technologies), rabbit polyclonal anti-human IL-1β (Clone 3553, Biovision) and goat anti-rabbit Alexa fluor 488 (Life technologies) were used for immunofluorescence detection of $CD4^{+}SLAMF7^{+}$ cells and IL-1β

producing $CD4^+$ cells in deparaffinized sections of tissue biopsies using established protocols.

In addition, three multi-color immunofluorescence staining panels CD4/SLAMF7/GATA-3, CD4/SLAMF7/IL-1β and CD4/ TGFβ1 were devised to measure the frequency and in vivo function $CD4^+SLAMF7^+$ CTLs. Detection was performed using mouse or rabbit Superpicture polymer detection kits (HRP; Life Technologies) followed by tyramide signal amplification by Opal 3-plex kit (Perkin Elmer) by following the manufacturer's protocol. The slides were counterstained with DAPI (Thermo Scientific) and mounted using Vectashield mounting medium (Vector labs). Stained tissues were scanned on TissueFAX (Tissuegnostics) and the frequency for $CD4^+$ cells co-expressing SLAMF7 and IL-1β was calculated using the proprietary TissueQuest software. The anti-IL-1β antibody used recognizes primarily the processed mature form of IL-1β.

Flow cytometric analysis: Fluorescence labeling for flow cytometry was performed by incubating cells in staining buffer (Biolegend) containing optimized concentrations of fluorochrome-conjugated antibodies. Except where indicated, all antibodies were procured from Biolegend. The following monoclonal antibodies were used in this study: anti-human CD19-Pacific Blue (clone HIB19), anti-human CD27-APC (clone O323), anti-human CD38-FITC (clone HIT2), anti-human IgG4 (clone 6025, Southern Biotech), anti-human CD4-PE-Cy7 (clone OKT4), anti-human CD8α-PE, anti-human CXCR5-PE (clone J252D4), CD39 (Clone A1), anti-human CD45RA-PE (clone HI100), anti-human CD45RO-APC (clone UCHL1), anti-human CD62L-FITC (clone DREG56), anti-human CD244-

biotin (clone C1.7, eBioscience), anti-human CD20-APC, anti-human CD319 (SLAMF7)-PE (clone 162.1), anti-human CD11b-APC Cy7 (clone ICRF44), anti-human CD28-PerCP Cy5.5 (clone CD28.2), anti-human TCR Vβ23 FITC (clone αHUT7), anti-human TCR Vβ17-PE (clone E17.5F3.15.13, Beckman-Coulter), anti-human TCR Vβ2-PE (clone MPB2D5, Beckman-Coulter), CD39-PE Cy7 (Clone A1, Biolegend) and CD25-APC Cy7 (Clone BC96, Biolegend). A table of concordance between the TCR Vβ gene nomenclatures and IMGT gene names, which is available on the IMGT website (http://www.imgt.org), was used to verify that the appropriate Vβ-specific antibody clones were selected to detect clonally-expanded T-cell clones identified by next-generation sequencing [56].

PBMCs and single cell suspensions from tissue biopsies were reacted with Fc blocking agent (Human FcX, Biolegend). Surface staining was performed using appropriate dilution of antibodies in 12x75mm round bottomed polystyrene tubes in the dark at 4°C. For intracellular staining (T-bet, GATA-3, Foxp3, granzyme B and perforin) cells were fixed and permeabilized with the Foxp3-staining kit (eBioscience) according to manufacturer's guidelines. Cells were then stained in permeabilization buffer with anti-human T-bet PECy7 (clone 4B10, eBioscience), GATA-3 PE-Cy7 (clone L50-823, BD Biosciences), anti-human FOXP3 Alexa Fluor 488 (Clone 206D, Biolegend), anti-human Perforin PE (clone B-D48) and anti-human granzyme B FITC (clone GB11). For the degranulation assay, $CD4^+SLAMF7^+$ CTLs were stimulated with 3 μg/mL anti-human CD3 (OKT3) for 4 hours and surface staining for anti-human CD107a (Biolegend) was performed

followed by permeabilization and intra-cellular staining for Granzyme B as discussed above.

EBV-transformed B cell lines from an IgG4-RD patient (P46) were used as targets in the allogeneic CTL assay. 5 x 10^4 EBV-transformed B cells were co-cultured for 12 hours with $CD4^+$ CTLs from two patients at different ratios in presence or absence of anti-CD3. Cells were harvested and surface stained for anti-human CD4 as described above followed by staining with Annexin V-APC in Annexin V binding buffer (15 minutes at room temperature). DAPI was added to the cells at a final concentration of 1 µg/ml. Target cells were gated as CD3-negative and percentage of apoptotic/dead cells were estimated by Annexin $V^+/DAPI^+$ gates.

Intracellular staining for cytokines in restimulated T cells: For detecting intracellular levels of cytokines, mononuclear cells were stimulated with 100 ng/mL of phorbol-myristoyl acetate (Sigma-Aldrich) and 100 ng/mL of ionomycin (Invitrogen) in the presence of Brefeldin A (Sigma-Aldrich) for 4 hrs at 37°C. They were subsequently labeled with the LIVE/DEAD* fixable violet viability dye (Invitrogen) in phosphate-buffered saline for 20 minutes and stained for cell surface markers. Cells were then fixed/permeabilized and stained with anti-human IFN-γ APC (clone 4S.B3), anti-human IL-4 Alexa Fluor® 488 (clone 8D4-8) for 45 minutes on ice. Cells were washed two times with permeabilization buffer and once with PBS and acquired/analyzed on a BD LSR II (BD

Biosciences). The .fcs files were analyzed using FlowJo software (version 9.6.3, Treestar).

Cell sorting: To preserve cell viability mononuclear cells were stained with relevant cell surface markers in DMEM (Gibco) with ITS+ Universal Culture Supplement (BD Biosciences). For batch sorts, antibody-stained cells were resuspended at ~20 million/mL in HBSS (Gibco) plus 10 mM glucose and sorted on a BD FACSAria II (BD Biosciences). Sorted cells were collected in 5 mL tubes containing 1 mL collection medium (DMEM with 30% FBS) and re-analyzed on the sorter to ensure > 99% purity in defined gates.

Deep sequencing analysis of TCR Vβ repertoire: Next-generation sequencing analysis of the TCR Vβ repertoire was undertaken using the ImmunoSeq® platform at Adaptive Biotechnologies Inc. at the "survey" level of sequencing depth, that is designed to target an output of 200,000 assembled output sequences after preprocessing filters [57, 58]. Briefly, genomic DNA was isolated from flow-sorted $CD4^+$ T cell subsets (T_{EM}, $CD4^+SLAMF7^+$ CTLs and GATA-3+ T_H2 cells) from individual IgG4-RD subjects. Sorted cell numbers ranged from ~5,000 to ~40,000, assuring at least 5-fold depth of sequencing. Genomic rearrangements of V-D-J gene segments at the TCRβ locus were amplified using multiplex PCR with forward and reverse primers specific for Vβ and Jβ gene segments respectively, and analyzed by paired-end Illumina sequencing. Use of barcoded primers allowed multiplexing of next-generation sequencing samples

on an Illumina Hi-Seq instrument. The sequences were assembled in silico, and V-D-J regions were reconstructed, following standard IMGT gene nomenclature for TCR Vβ gene segments [56]. Non-productive rearrangements were excluded from the analysis.

Gene-expression analysis: The nCounter® human immunology panel (NanoString Technologies), comprising ~500 immunology-related genes was used to quantify the gene expression of effector/memory T cells in IgG4-RD. RNA was extracted from 10,000-50,000 flow-sorted T cells using the Qiagen RNAEasy Micro kit according to manufacturer's protocol. Targets were reverse-transcribed and pre-amplified for 14 cycles using the standard multiplexed target enrichment (MTE) protocol (NanoString Technologies) for 458 target genes, which has been previously validated to yield a linear response. The amplified products were hybridized in solution to color-coded nCounter capture and reporter probes and captured on an nCounter Cartridge for high-resolution digital scanning and analysis on the GEN2 Digital Analyzer at NanoString Technologies. The raw gene expression data was normalized to the mean of the spiked-in internal positive control probes to correct for technical assay variation and subsequently normalized to the mean of 15 housekeeping genes included in the nCounter codeset to correct for differences in sample input or variation in reverse-transcription/pre-amplification. Biological replicates were evaluated for consistency and differential expression analysis of gene expression was undertaken using the ComparativeMarkerSelection module in the GenePattern pipeline (version 3.5.0) [59, 60].

Quantitative real time PCR: Total RNA was extracted from ~10,000 – 40,000 cells using the RNAeasy plus Micro kit (Qiagen). cDNA was synthesized using a RT2 first-strand kit (Qiagen) followed by quantitative real time PCR analysis (SYBR green; Life technologies). GAPDH mRNA expression was used as the normalizing control. The primers used were:

ThPOK (F: 5'-gtctgccacaagatcatcca-3', R: 5'-tcgtagctgtgcaggaagc-3'),

Runx3 (F:5'cagaagctggaggaccagac-3', R: 5'-gtcggagaatgggttcagtt-3') &

GAPDH (F: 5'-atgttcgtcatgggtgtgaa-3', R: 5'-gtcttctgggtggcagtgat-3')

ELISpot and western blotting for IL-1β: Prior to coating, 96-well polyvinylidene difluoride (PVDF) membrane plates (Millipore) were prewet with 50ul 70% ethanol/well for 2 minutes and washed three times with 200ul sterile filtered water. ELISpot assay for IL-1β was performed using human IL-1β ELISpot Ready-SET-Go kit (eBioscience) according to the manufacturer's recommendations. In brief, plates were coated overnight at 4°C with the anti-human IL-1β antibody provided, followed by gentle washing with ELISpot wash buffer (1X PBS plus 0.05% Tween-20) and blocking with complete medium (RPMI plus 10% fetal bovine serum) for 2 hours at room temperature. 10000 sorted $CD4^+CD45RO^+$ cells from healthy controls and IgG4-RD patients were rested on the plate in complete medium for 4 hours post-sorting, and stimulated with PMA (100ng/ml) and ionomycin (100ng/ml) overnight at 37°C. Cells were decanted gently using wash buffer to detach any adherent cells and plates were washed three times with wash buffer followed by incubation with the

recommended dilution of biotinylated detection antibody for 2 hours at room temperature. After two additional washes, plates were incubated with horse-radish peroxidase conjugated with streptavidin for 45 minutes at room temperature. The plates were washed extensively 4 times with wash buffer followed by two additional washes with PBS to remove any traces of tween-20. 100 µL of TMB substrate (MabTech) was added and spots were allowed to develop for upto 20 minutes. Counting and visual analysis of the spots were done using a computer-operated CTL ELISpot reader and the fraction of IL-1β secreting cells was quantified as the number of spots detected per 10,000 cells applied to the well.

For Western blot analysis of secreted IL-1β, $CD4^+CD45RO^+$ cells from healthy donors, $CD4^+CD27^-$ gated $SLAMF7^+$ and $SLAMF7^-$ cells from an IgG4-RD subject were sorted and expanded in vitro in a U-bottomed 96-well plate (BD Falcon) with weekly anti-CD3 stimulation (Biolegend; OKT3, 3µg/ml) in media supplemented with 10ng/mL of rhIL-2. 150,000 cells were re-stimulated with anti-human CD3 (Biolegend; OKT3, 3µg/ml) or Lipopolysaccharide (LPS; Sigma, 5µg/ml) and the culture supernatants were harvested at 60hrs. These supernatants were run on an SDS-PAGE gel and transferred onto Immobilon-P membranes. IL-1β was detected using a rabbit anti-human IL-1β antibody (Biovision) followed by goat anti-rabbit Ig-HRP (Thermo scientific) and developed using SuperSignal West Pico Chemiluminescent Substrate (Biorad). LPS stimulated PBMCs were used as positive controls.

ELISA for TGF 1: $CD4^+$ CTLs and $CD4^+CD45RA^+$ naïve cells from IgG4-RD patients were stimulated in vitro in 96 well plates (50,000 cells/well) with anti-human CD3 (Biolegend; OKT3, 3µg/ml) in media supplemented with 10ng/mL of rhIL-2 and the culture supernatants were harvested at 48hrs. ELISA was performed on these culture supernatants using a Human TGFβ1 Quantikine ELISA kit using the manufacturer's protocol. Standards provided in the kit were used to quantify TGFβ1 in culture supernatants.

SUPPLEMENTARY FIGURE LEGENDS

Figure E1: Abundance of $CD4^+GATA3^+$ Th2 cells in IgG4-RD patients

(A) Representative plot for GATA-3 expression in $CD4^+CD45RA^-$ gated cells from patients with IgG4-RD compared with a healthy control.
(B) The frequency of $CD4^+GATA\text{-}3^+$ TH2 cells in atopic and non-atopic subsets of IgG4-RD subjects compared to healthy controls (p-values for unpaired t-tests are shown; error bars represent the standard deviation).

Figure E2. Expanded $CD4^+CD27^-CD62L^-$ cells are $CD45RO^+$

CD45RO levels on $CD4^+CD27^-CD62L^-$ from 4 index patients P2, P12, P19 and P25

Fig E3: Abundance of regulatory T cells in peripheral blood of IgG4-RD patients

The numbers of $CD4^+CD45RO^+CD39^+CD25^+Foxp3^+$ Treg cells in peripheral blood of IgG4-RD subjects. P values are based on the Mann-Whitney test.

Figure E4. In vitro culture of $CD4^+$ CTLs from PBMCs of an IgG4-RD subject

Flow-sorted $CD4^+SLAMF7^+$ CTLs from an IgG4-RD patient were stimulated with anti-human CD3 and anti-human CD28 beads in presence of recombinant human IL-2 (20 ng/mL) and their phenotype was checked after 2 weeks of culture.

Figure E5: $CD4^+$ CTLs show surface expression of CD8~

Gating strategy to depict the CD8α expression on $CD4^+$T-bet^+ CTLs from a representative patient (P25).

Figure E6. CD4+ CTLs from IgG4-RD patients are functional killer cells

The cytotoxicity of in vitro expanded $CD4^+$ CTLs derived from two subjects (P11 and P31) and $CD4^+CD45RO^+$ cells derived from a healthy control against an allogeneic EBV-transformed B cell target cell line was measured after 12 hours of co-culture with or

without anti-CD3 (10 μg/mL) using Annexin V staining at varying $CD4^+$ CTL: target ratios.

Figure E7. The TCR V repertoire of expanded T_{EM} cells in IgG4-RD

(A) Cumulative distribution of clone frequencies in $CD4^+$ T_{EM} cells from the 4 IgG4-RD subjects and 4 healthy controls in (A**)**. The minimum number of clones accounting for 10% (D10) and 50% (D50) of the clonal diversity are shown in the table below.

(B) Flow cytometry gating scheme used to validate the dominant expanded T_{EM} clones identified by next-generation sequencing (subject P25 shown).

(C) Vβ-specific antibodies were used to compare the frequencies of the dominant T_{EM} clones identified in subjects P25, P28 and P31, marked with a red boundary in (A), with the background frequencies found in controls and non-T_{EM} cells in the respective patients.

Figure E8. Increased frequency of $CD4^+SLAMF7^+$ CTLs in peripheral blood of IgG4-RD patients

Frequency of total $CD4^+SLAMF7^+$ CTLs in IgG4-RD subjects (n = 101) compared to healthy controls (n = 35). **Mann-Whitney test, $p < 0.05$.

Figure E9: Abundance of $CD4^+SLAMF7^+$ CTLs in atopic vs non-atopic IgG4-RD patients

The frequency of $CD4^+SLAMF7^+$ CTLs in atopic and non-atopic subsets of IgG4-RD subjects compared to healthy controls (p-values for unpaired t-tests are shown; error bars represent the standard deviation).

Figure E10. Expansion of $CD4^+SLAMF7^+$ CTLs in disease lesions of IgG4-RD subjects.

(A) Immunofluorescence staining of $CD4^+SLAMF7^+$ CTLs in the affected tissues of IgG4-RD subjects (lacrimal gland biopsy from P3, lymph node biopsy from P11, submandibular salivary gland P25, laryngeal biopsy from P27, nasal palate biopsy from P31, retroperitoneal biopsy from P40 and nasal septum biopsy from P43). CD4 (red), DAPI (blue) and SLAMF7 (green) staining are shown.
(B) Immunofluorescence staining of an affected submandibular salivary gland from an IgG4RD subject (P25) for CD4, Vβ17 (red) and SLAMF7 (green) shown both individually and as an overlay.

Figure E11. $CD4^+SLAMF7^+$ CTLs express granzyme A in disease lesions of IgG4-RD subjects.

(A) Immunofluorescence staining for granzyme A on $CD4^+SLAMF7^+$ CTLs in the affected tissues of IgG4-RD subjects (lymph node biopsy from P11, nasal palate biopsy from P31, retroperitoneal biopsy from P32). CD4 (red), DAPI (blue), SLAMF7 (green) and Granzyme A (magenta) stainings are shown.

Figure E12. Expanded $CD4^+$ CTLs clones from IgG4-RD patients secrete IFN-γ

Intracellular staining for IFN-γ and IL-4 in expanded clones of $CD4^+$ CTLs identified using Vβ and T-bet staining from two IgG4-RD patients after restimulation with PMA (100 ng/mL) and ionomycin (100 ng/mL).

Figure E13. Expanded $CD4^+$ CTLs from IgG4-RD patients secrete IL-1β.

IL-1β-producing $CD4^+$ cells in the tissues of IgG4-RD subjects and controls. CD4 (red), DAPI (blue) and IL-1β (green) staining are shown.

Figure E14. Expanded $CD4^+$ CTLs from IgG4-RD patients secrete TGF-s a

TGF-β1-producing $CD4^+GzmA^+$ cells in the salivary gland tissues of 5 IgG4-DS subjects and 5 controls (SS patients). CD4 (red), TGF-β1(white), DAPI (blue) and Granzyme A (green) staining are shown.

Figure E15. The rituximab target CD20 is not expressed on $CD4^+$ $SLAMF7^+$ CTLs

Flow cytometry revealed no detectable CD20 on CD4+CTLs. Three subjects (P25, P27 and P49 are shown).

Figure E16. Expansion of $CD4^+SLAMF7^+$ CTLs in subjects with systemic sclerosis.

Expansion of $CD4^+SLAMF7^+$ CTLs in patients with systemic sclerosis (n = 17). Patients with diffuse scleroderma (n = 8) and limited scleroderma (n = 9) are also shown separately. Boxplots display the 25^{th} to 75^{th} percentiles. P values are based on the Mann-Whitney test.

SUPPLEMENTARY TABLE E1:
Clinical features of scleroderma patients studied.

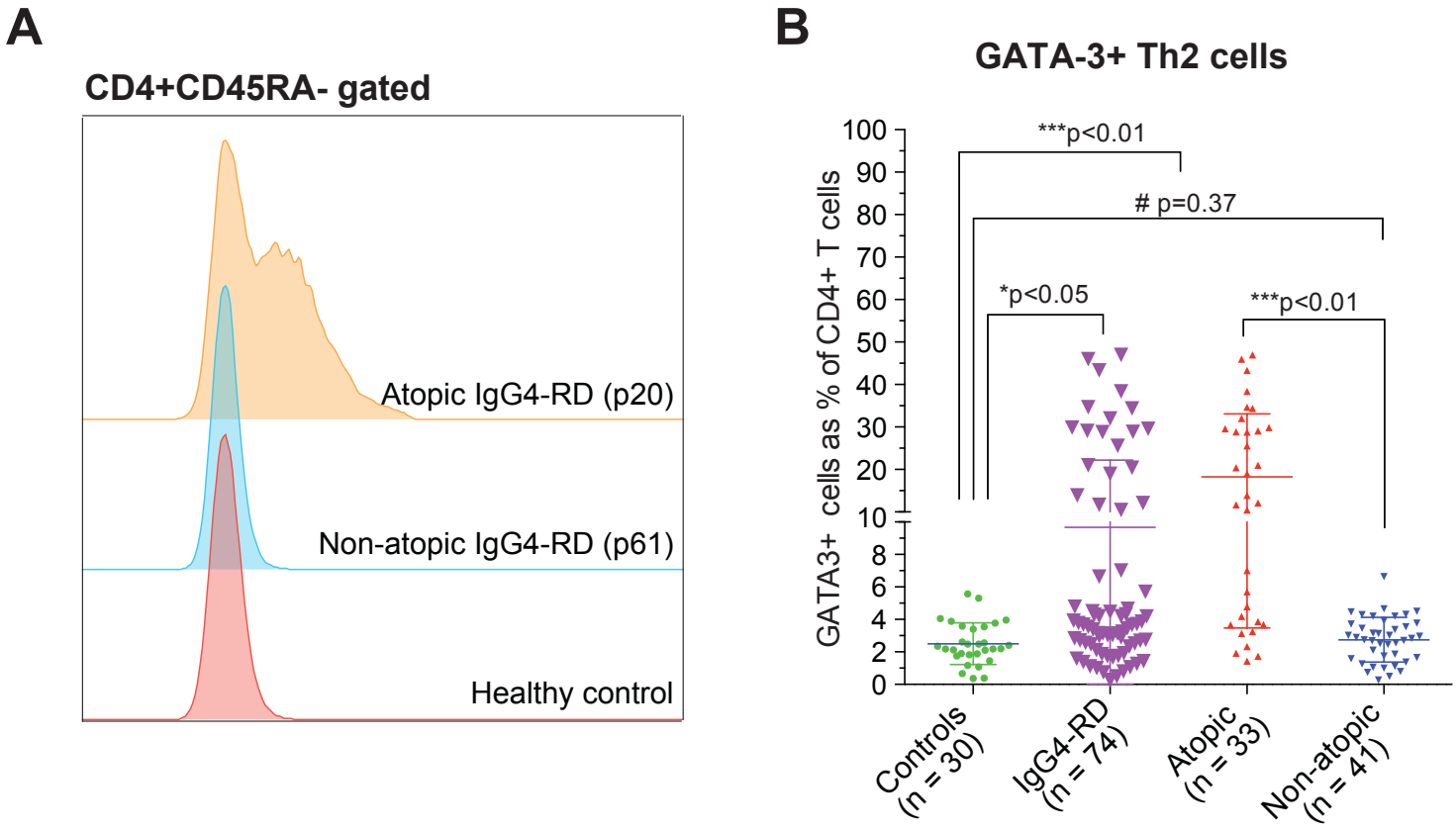
Type	Time since diagnosis	Organ involvement	Treatment	Serologies
Diffuse	40 months	Raynaud's, interstitial lung disease, skin	Mycophenolate mofetil	ANA (pattern unknown), RNP, Scl70
Diffuse	12 months	Skin, esophageal dysfunction, GERD, sclerodactyly	Hydroxychloroquine	ANA (speckled), Ro, La
Limited	120 months	Raynaud's, cutaneous & lingual telangiectasias, digital ulcers, bowel hypomotility	Calcium channel blockers, sildenafil	ANA (centromere)
Diffuse	108 months	Erosive synovitis (RA), sclerodactyly, telangiectasias, myopericarditis, restrictive lung disease	Methotrexate	ANA (nuclear), Ro, RF, CCP
Limited	126 months	Raynaud's, gastric antral vascular ectasia, facial telangiectasias, microscopic colitis	None	ANA (centromere)
Limited	84 months	Raynaud's, esophageal dysfunction, GERD	None	ANA (centromere), dsDNA (low titer)
Diffuse	36 months	Raynaud's, sclerodactyly, interstitial lung disease, inflammatory myopathy	Glucocorticoids, azathioprine	ANA (nucleolar)
Diffuse	60 months	Interstitial lung disease, mild pulmonary hypertension, skin thickening, sclerodactyly, capillary loop dropout	None	ANA (speckled)
Limited	180 months	Raynaud's, facial telangiectasias	Hydroxychloroquine	ANA (centromere)
Limited	36 months	Interstitial lung disease, GERD		ANA (centromere)
Limited	132 months	morphea, secondary Sjogren's	None	ANA (centromere)
Limited	24 months	Raynaud's, cutaneous telangiectasias	None	ANA (centromere)
Limited	Unknown	Raynaud's, narrowing of oral aperture, sclerodactyly	None	ANA (speckled)
Diffuse	4 months	Skin thickening	Methotrexate	ANA (homogeneous)
Limited	84 months	Raynaud's, calcinosis cutis, telangiectasias, esophageal dysmotility	None	ANA (centromere)

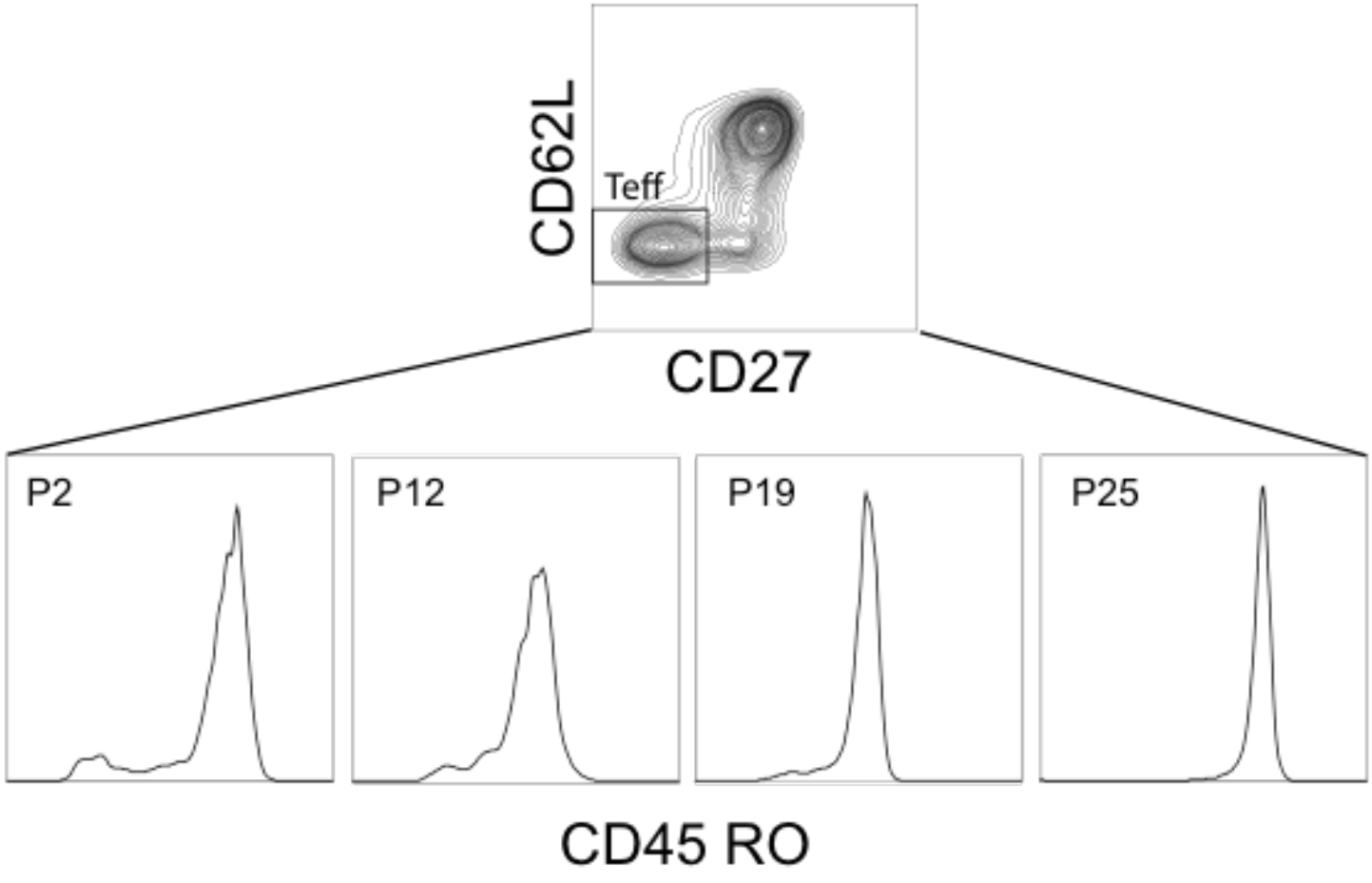
Diffuse	24 months	Diffuse skin thickening, sclerodactyly, Raynaud's, hypopigmentation, gastrointestinal dysmotility, diffuse rash, photosensitivity, alopecia,	Hydroxychloroquine, prednisone, azathioprine	ANA (pattern unknown)

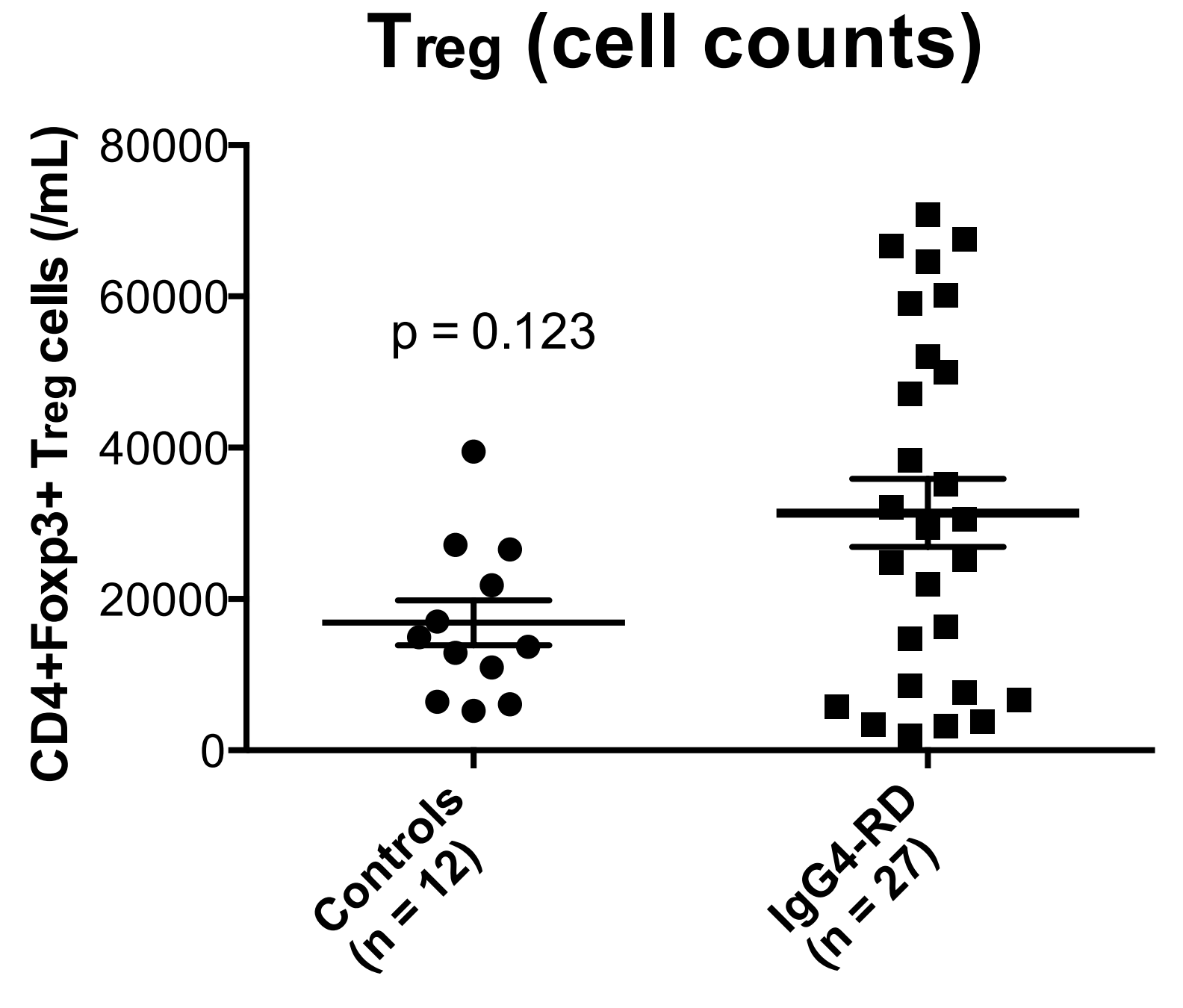
286
287

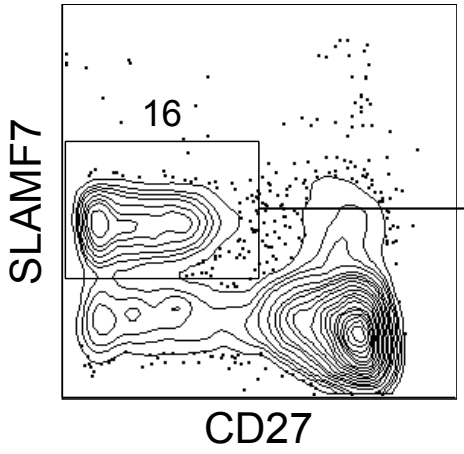
Supplementary table E2. Categorization of IgG4-RD patients into Atopic vs Non-atopic.

	Atopic patients (n=33)	Non-atopic patients (n=41)	All patients (n=74)
Mean age in years (range)	57.9 (30-84)	62.75 (33-88)	60.6 (30-88)
Male / Female ratio	2.3	1.732	2.1
Atopic symptoms, n (%)			
Rhinitis	18 (55%)		
Conjunctivitis	5 (7%)		
Asthma	9 (27%)		
Hives	3 (12%)		
Oral allergic syndrome	1 (3%)		
Eczema	2 (6%)		
Hay fever	2 (6%)		
Anaphylaxis	0		
Laboratory analysis, mean (range)			
Eosinophils (cells/mL) (< 500 cells/μL)	615 (40-1850)	316 (10-2000)	445 (10-1850)
Serum IgE (IU/mL) (< 100 IU/mL)	446 (5-1860)	236 (5-4570)	333 (5-1860)
Serum IgG4 (mg/dL) (< 121 mg/dL)	716 (11-4780)	273 (3-2200)	471 (3-4780)
Eosinophilia	(15/33)(45%)	(7/41)(17%)	(22/74)(17%)
Elevated IgE	(20/33)(61%)	(6/41)(15%)	(26/74)(15%)
Elevated IgG4	(26/33)(79%)	(12/41)(29%)	(38/74)(29%)


A
CD4+CD45RA- gated
Atopic IgG4-RD (p20)
Non-atopic IgG4-RD (p61)
Healthy control
B
GATA-3+ Th2 cells
GATA3+ cells as % of CD4+ T cells
***p<0.01
p=0.37
*p<0.05
***p<0.01
Controls (n = 30)
IgG4-RD (n = 74)
Atopic (n = 33)
Non-atopic (n = 41)


CD62L
Teff
CD27
P2
P12
P19
P25
CD45 RO


Treg (cell counts)
CD4+Foxp3+ Treg cells (/mL)
80000
60000
40000
20000
0
p = 0.123
Controls
(n = 12)
IgG4-RD
(n = 27)



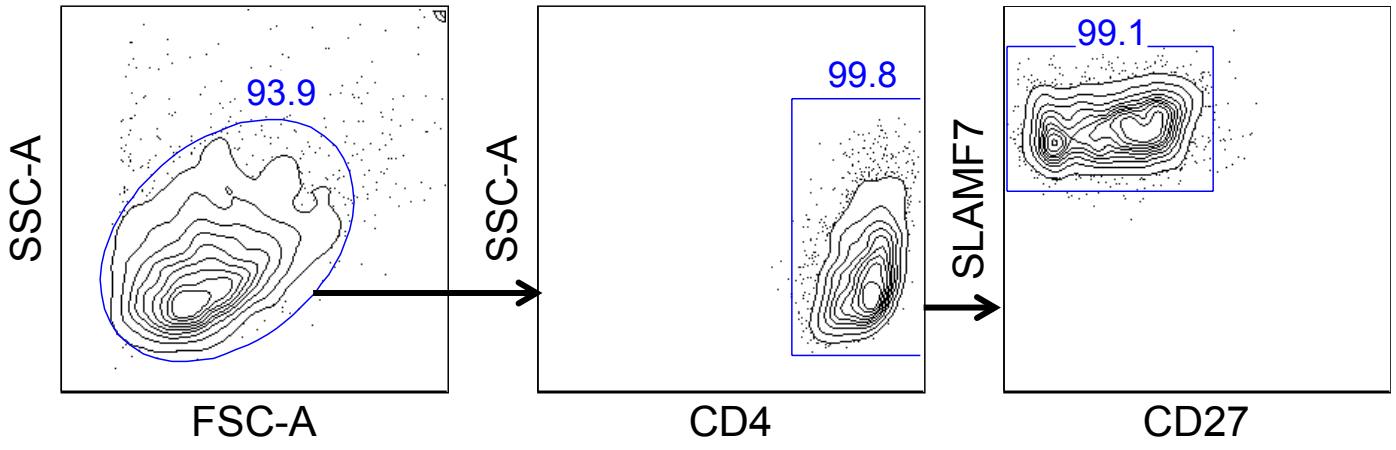
FACS SORT

↓

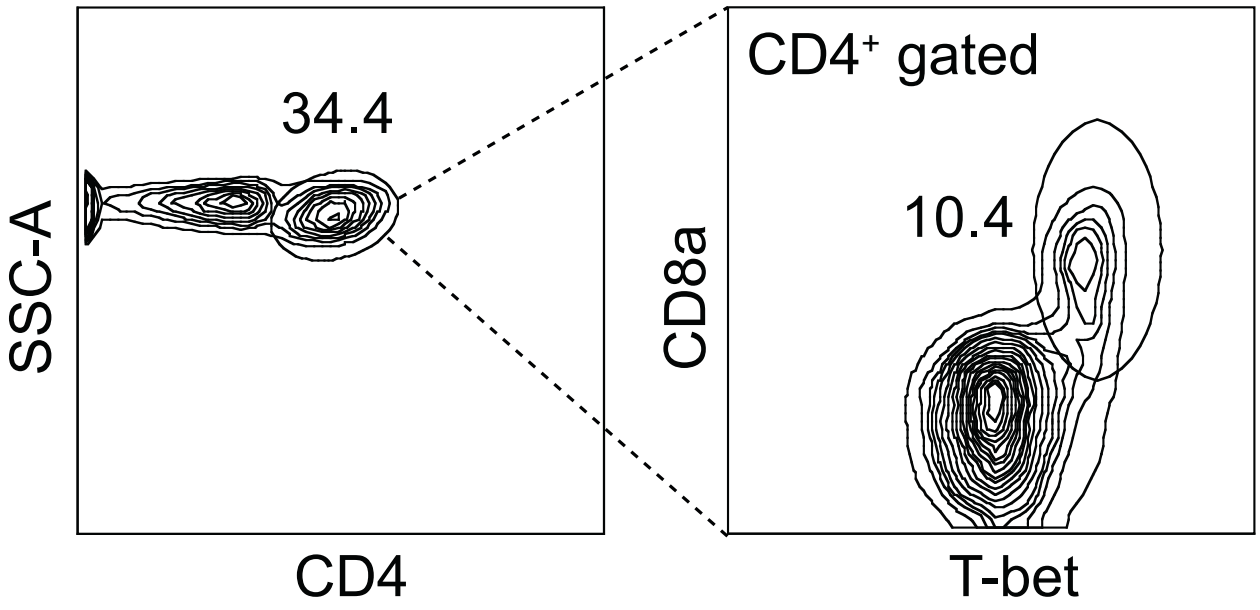
αCD3 + αCD28

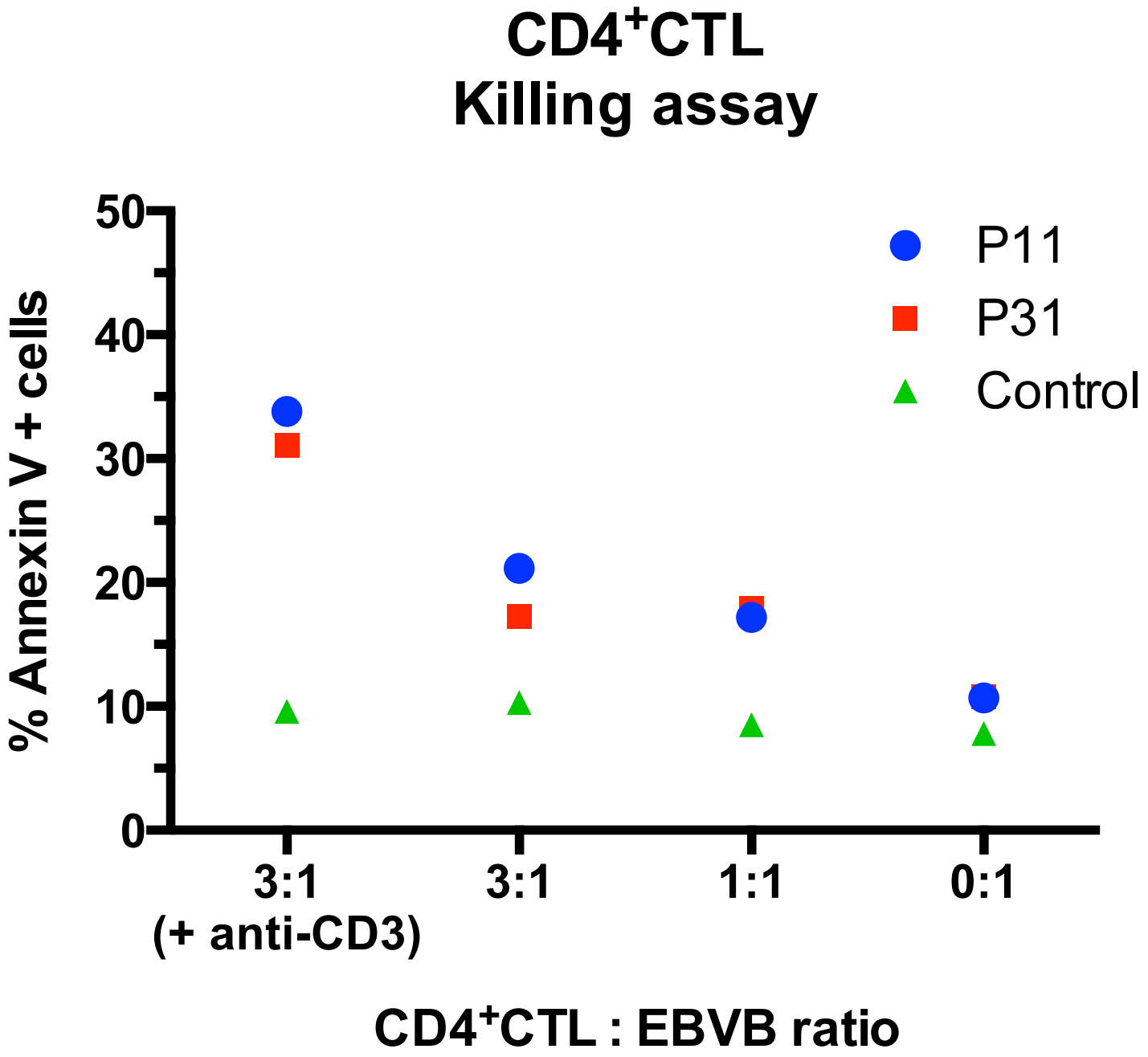
↓

2 WEEK CULTURE IN IL-2

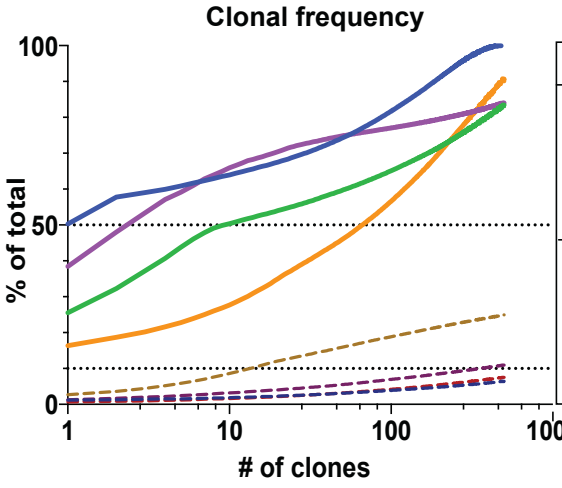


~ 50 FOLD INCREASE IN CELL NUMBER


34.4
SSC-A
CD4
CD4+ gated
10.4
CD8a
T-bet

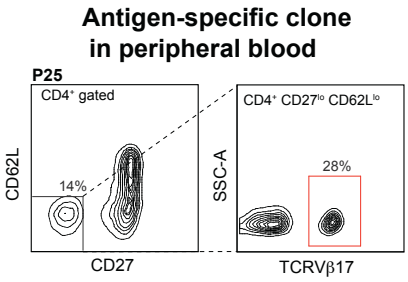

CD4+CTL
Killing assay
% Annexin V + cells
50
40
30
20
10
0
P11
P31
Control
3:1
(+ anti-CD3)
3:1
1:1
0:1
CD4+CTL : EBVB ratio

A

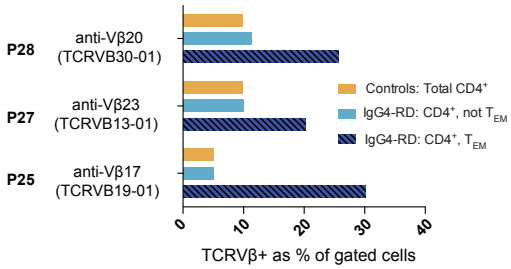


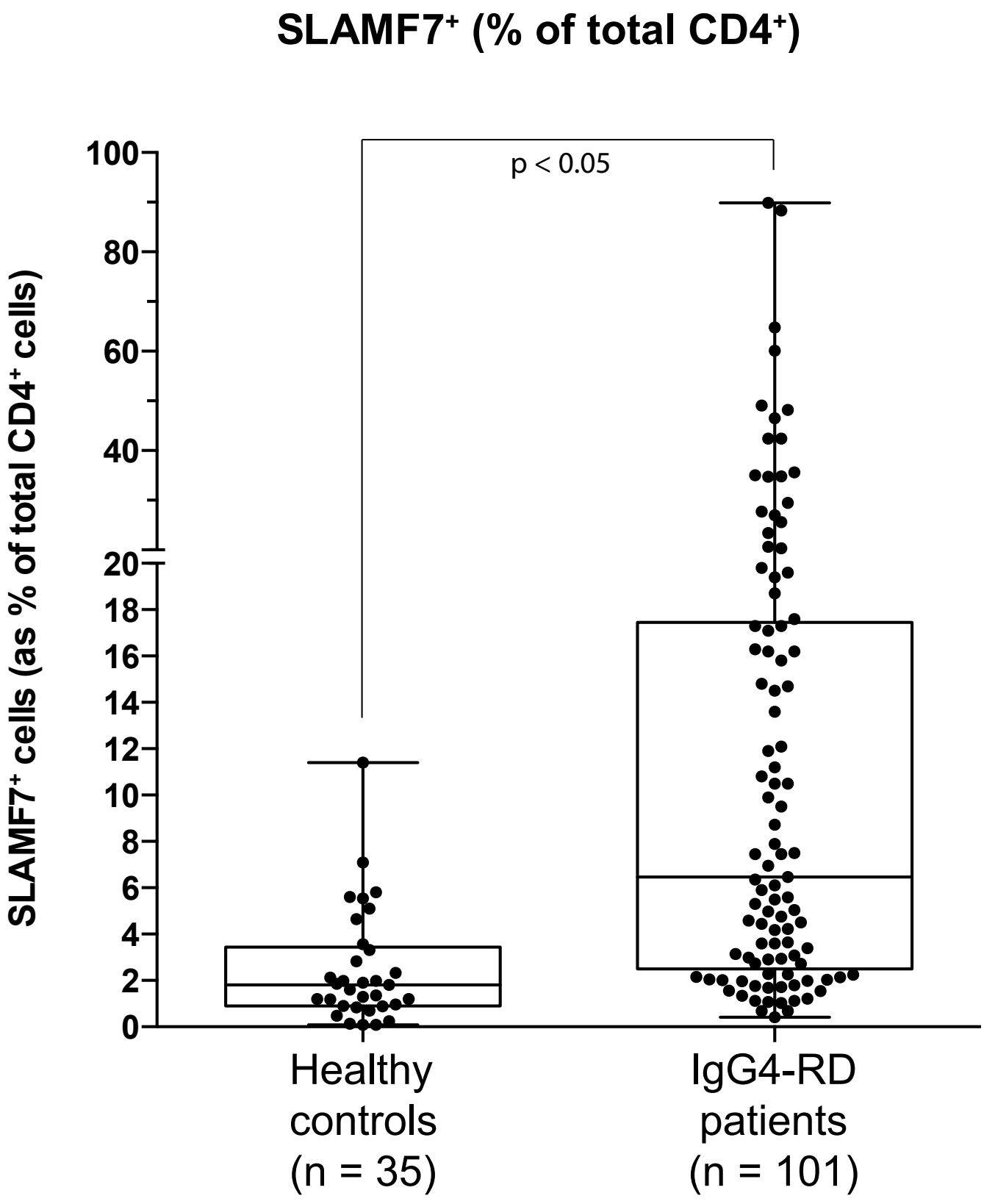
	D10	D50
P25	1	1
P27	1	11
P28	1	3
P31	1	68
Ctrl1	15	>10000
Ctrl2	1806	>20000
Ctrl3	502	>20000
Ctrl4	1143	>20000

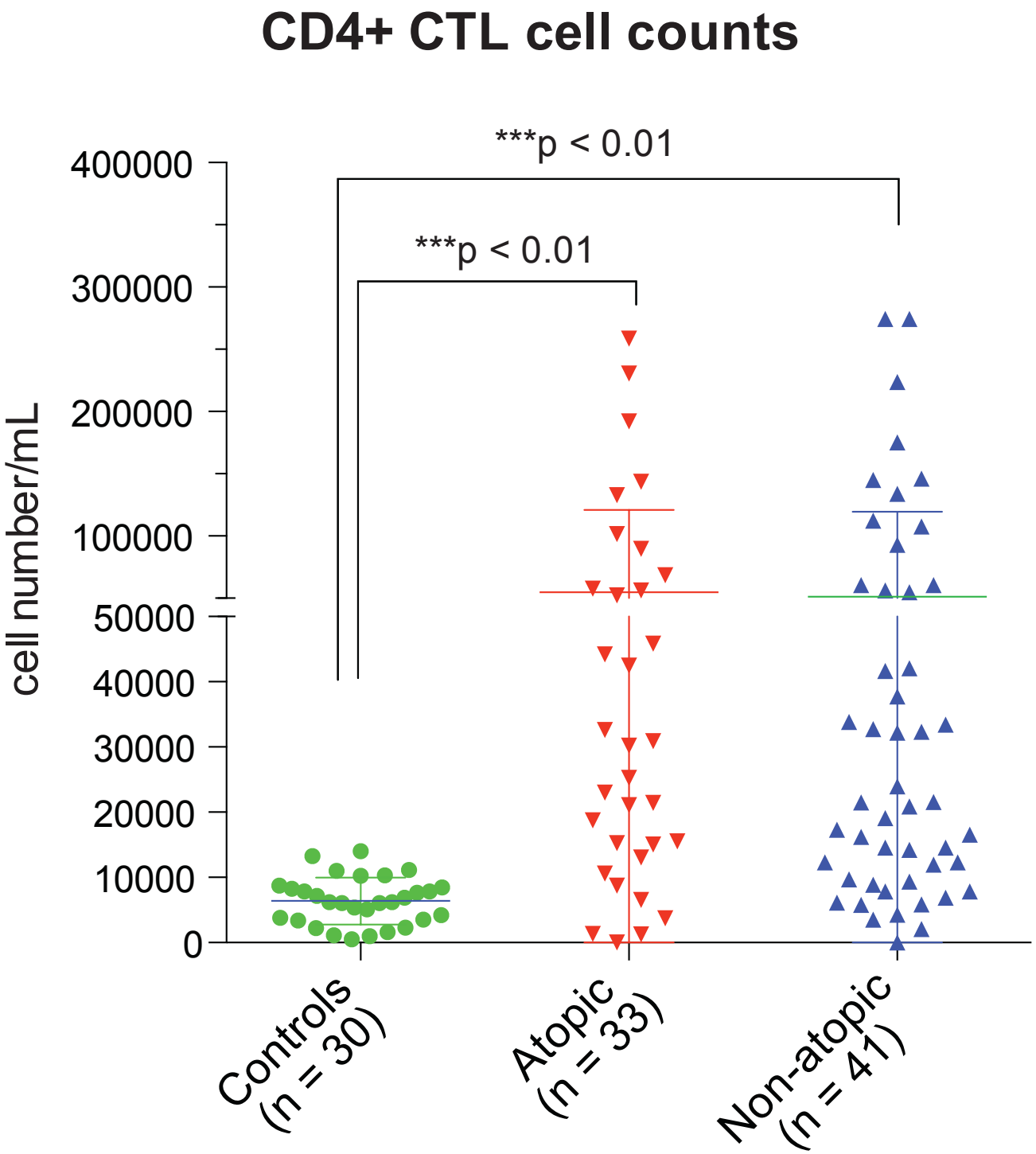
B

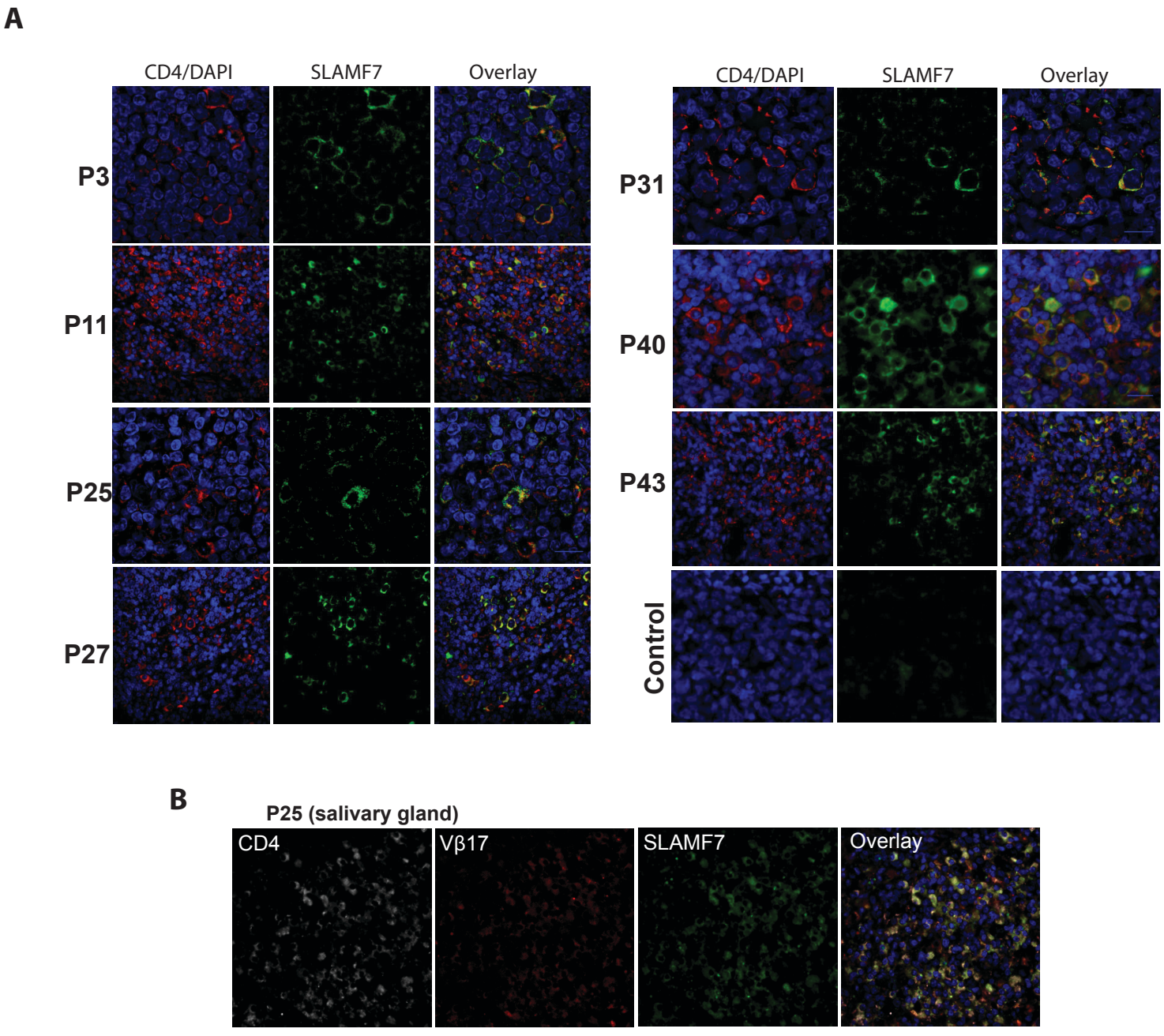


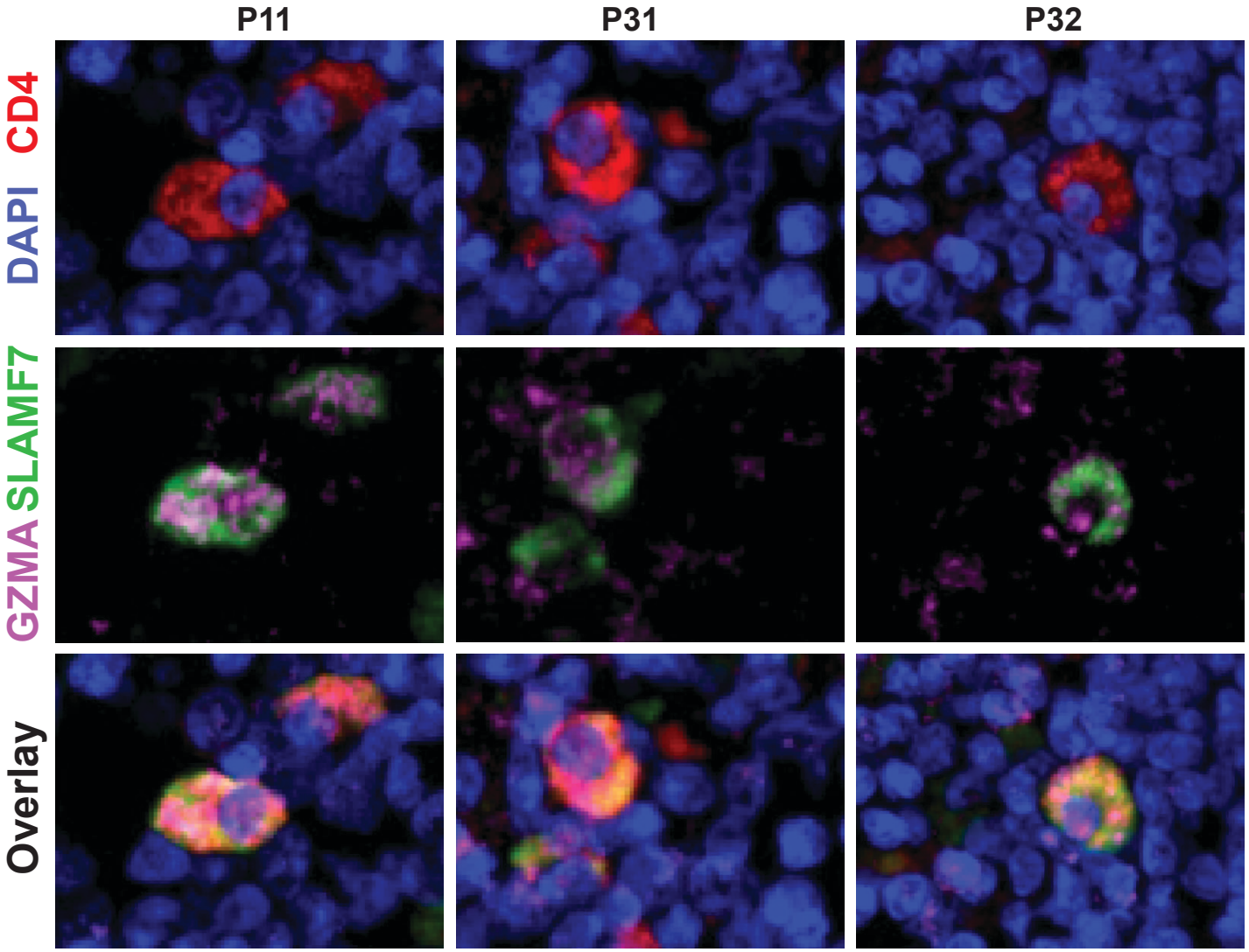
C

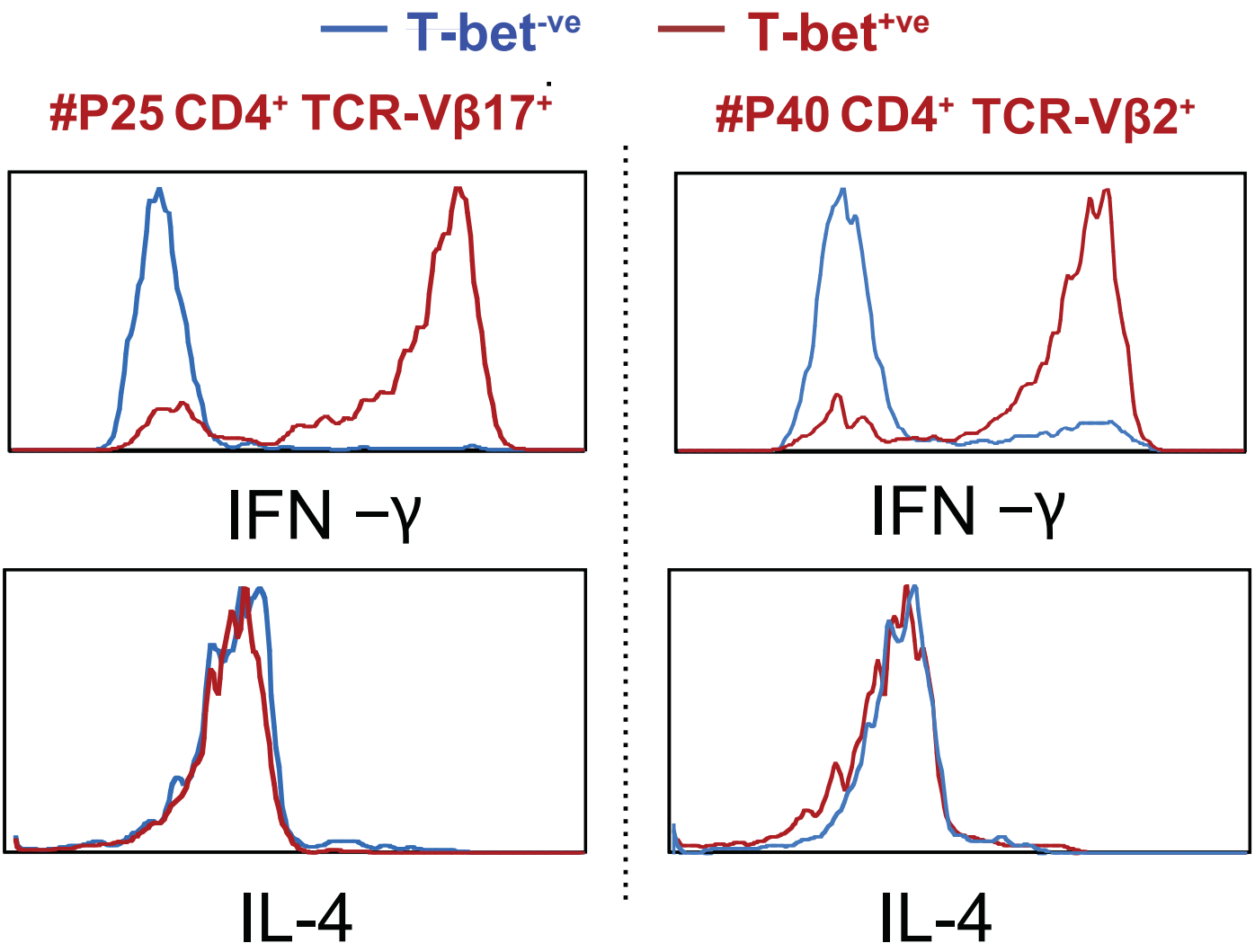


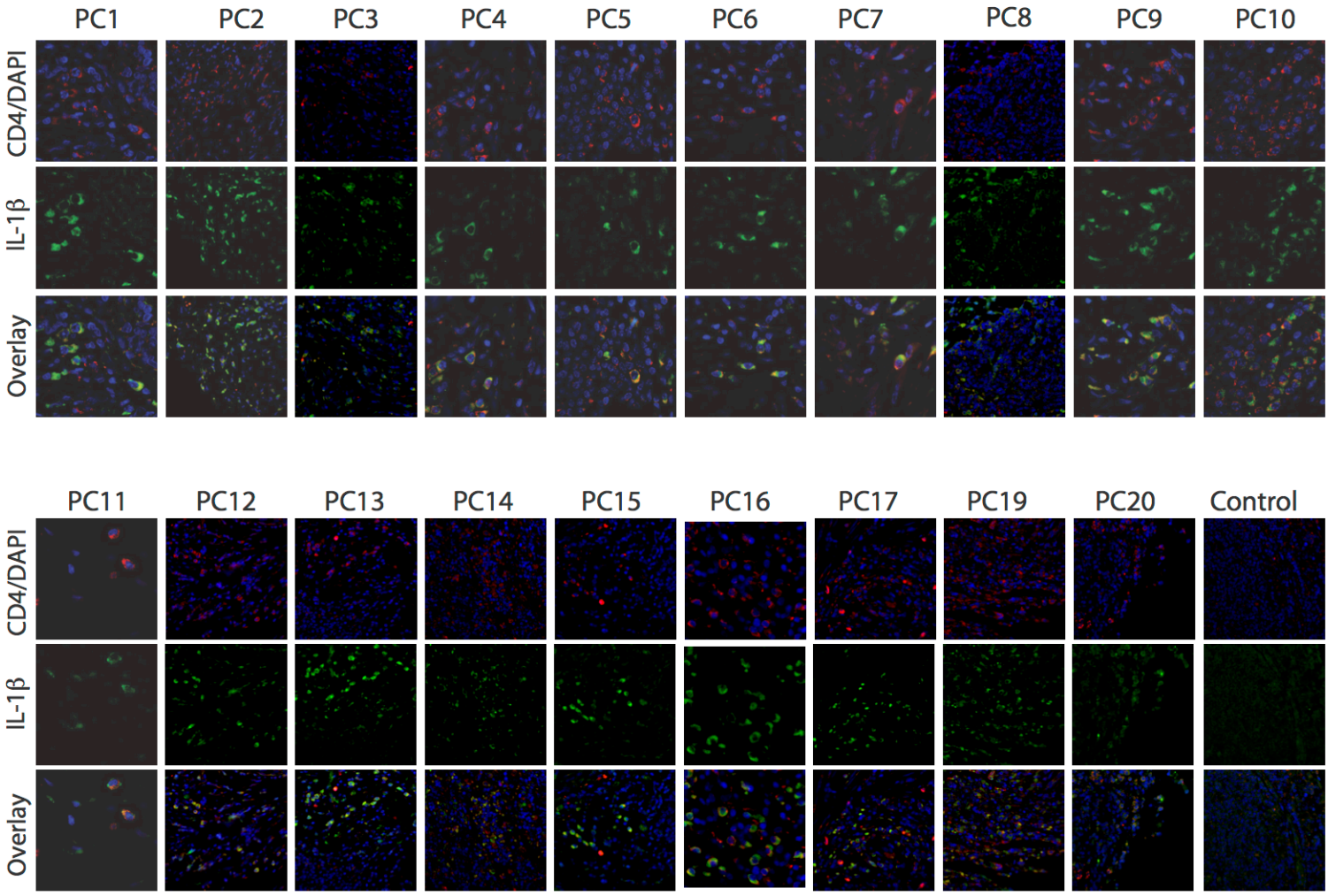

SLAMF7+ (% of total CD4+)
SLAMF7+ cells (as % of total CD4+ cells)
p < 0.05
100
80
60
40
20
18
16
14
12
10
8
6
4
2
0
Healthy controls (n = 35)
IgG4-RD patients (n = 101)

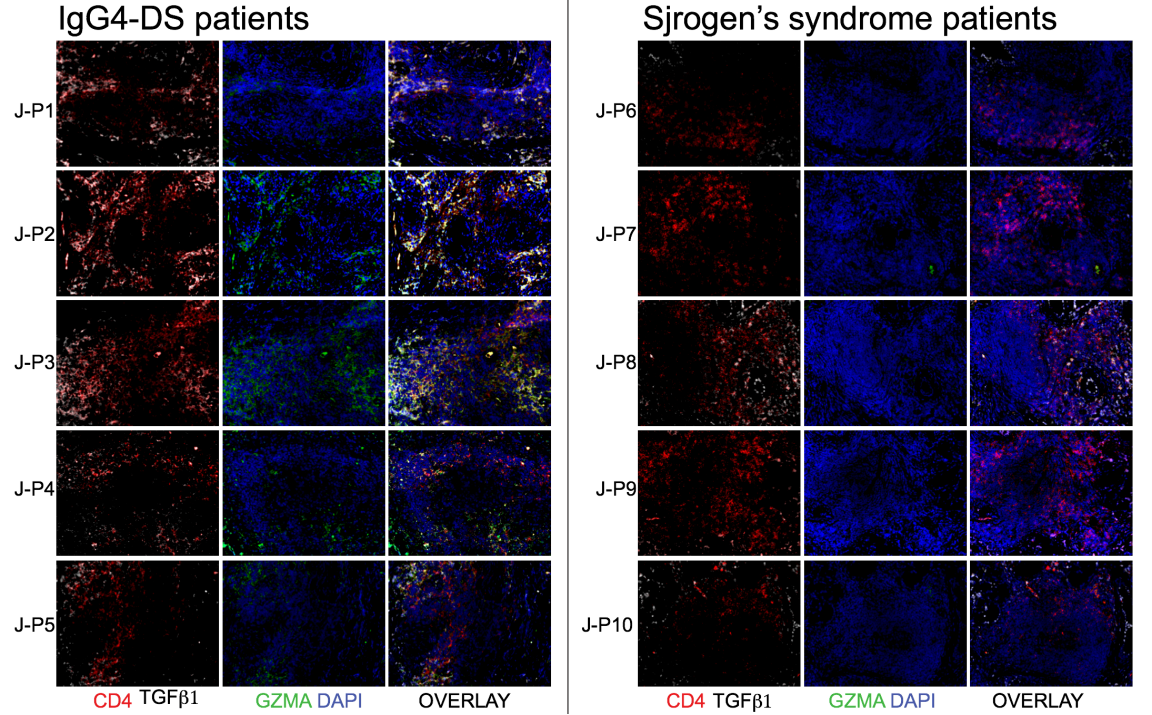

CD4+ CTL cell counts
***p < 0.01
***p < 0.01
cell number/mL
400000
300000
200000
100000
50000
40000
30000
20000
10000
0
Controls (n = 30)
Atopic (n = 33)
Non-atopic (n = 41)

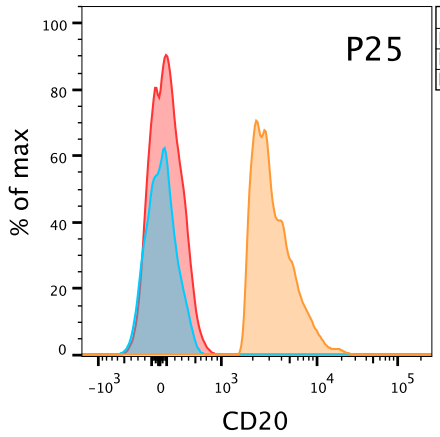

A
CD4/DAPI
SLAMF7
Overlay
P3
P11
P25
P27
P31
P40
P43
Control
B
P25 (salivary gland)
CD4
Vβ17
SLAMF7
Overlay


P11
P31
P32
DAPI CD4
GZMA SLAMF7
Overlay

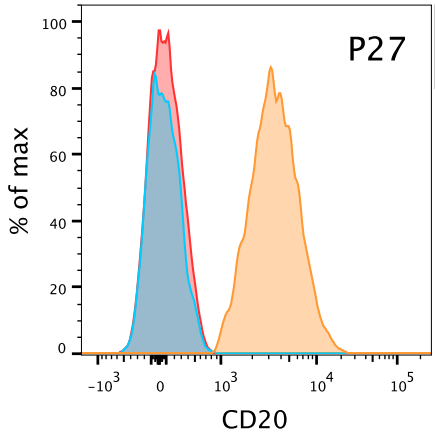

T-bet-ve
T-bet+ve
#P25 CD4+ TCR-Vβ17+
#P40 CD4+ TCR-Vβ2+
IFN −γ
IFN −γ
IL-4
IL-4


PC1
PC2
PC3
PC4
PC5
PC6
PC7
PC8
PC9
PC10
CD4/DAPI
IL-1β
Overlay
PC11
PC12
PC13
PC14
PC15
PC16
PC17
PC19
PC20
Control
CD4/DAPI
IL-1β
Overlay

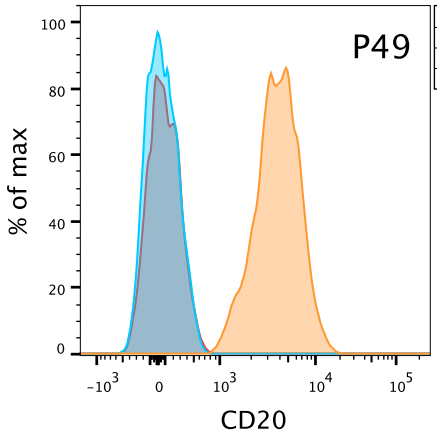

IgG4-DS patients
Sjrogen's syndrome patients
J-P1
J-P2
J-P3
J-P4
J-P5
J-P6
J-P7
J-P8
J-P9
J-P10
CD4 TGFβ1
GZMA DAPI
OVERLAY
CD4 TGFβ1
GZMA DAPI
OVERLAY



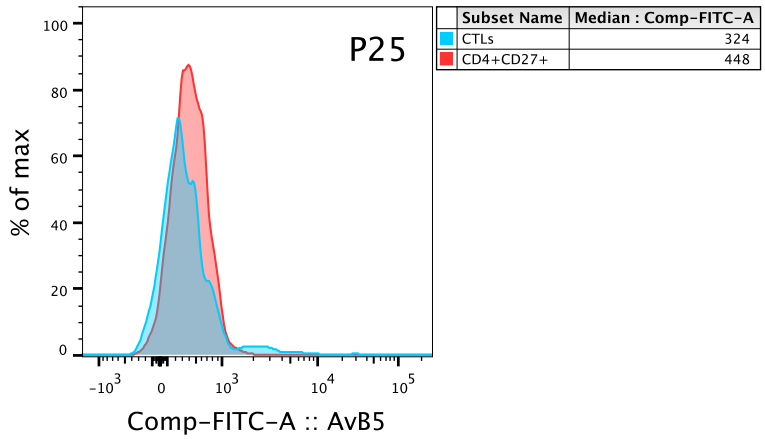
	Subset Name	Median : Comp-FITC-A
	B cells	1664
	CTLs	324
	CD4+CD27+	448



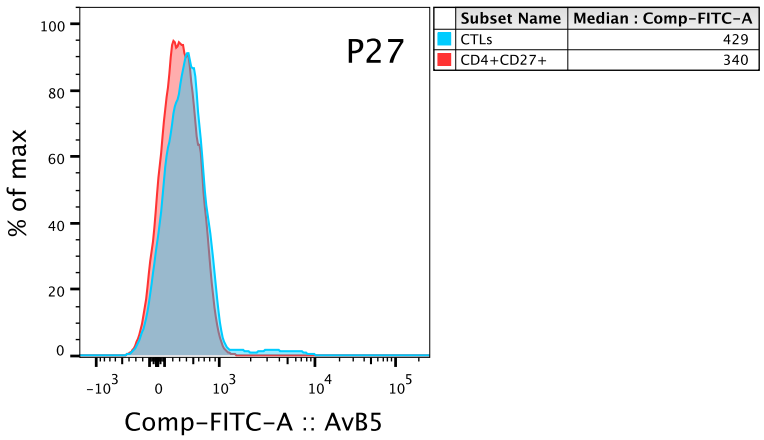
	Subset Name	Median : Comp-FITC-A
	B cells	1168
	CTLs	429
	CD4+CD27+	340



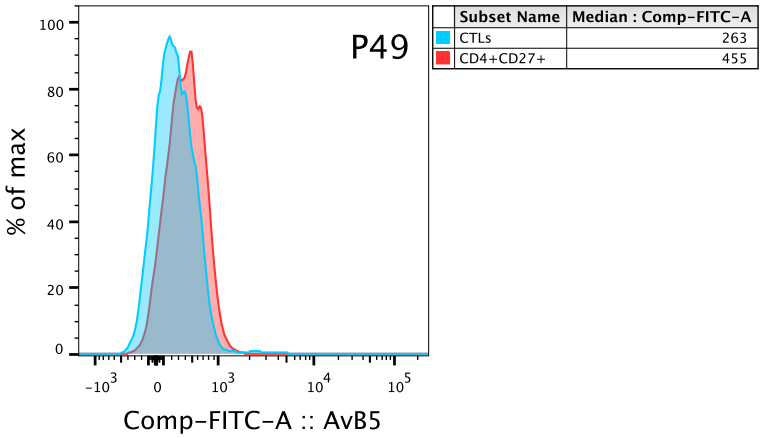
	Subset Name	Median : Comp-FITC-A
	B cells	1112
	CTLs	263
	CD4+CD27+	455



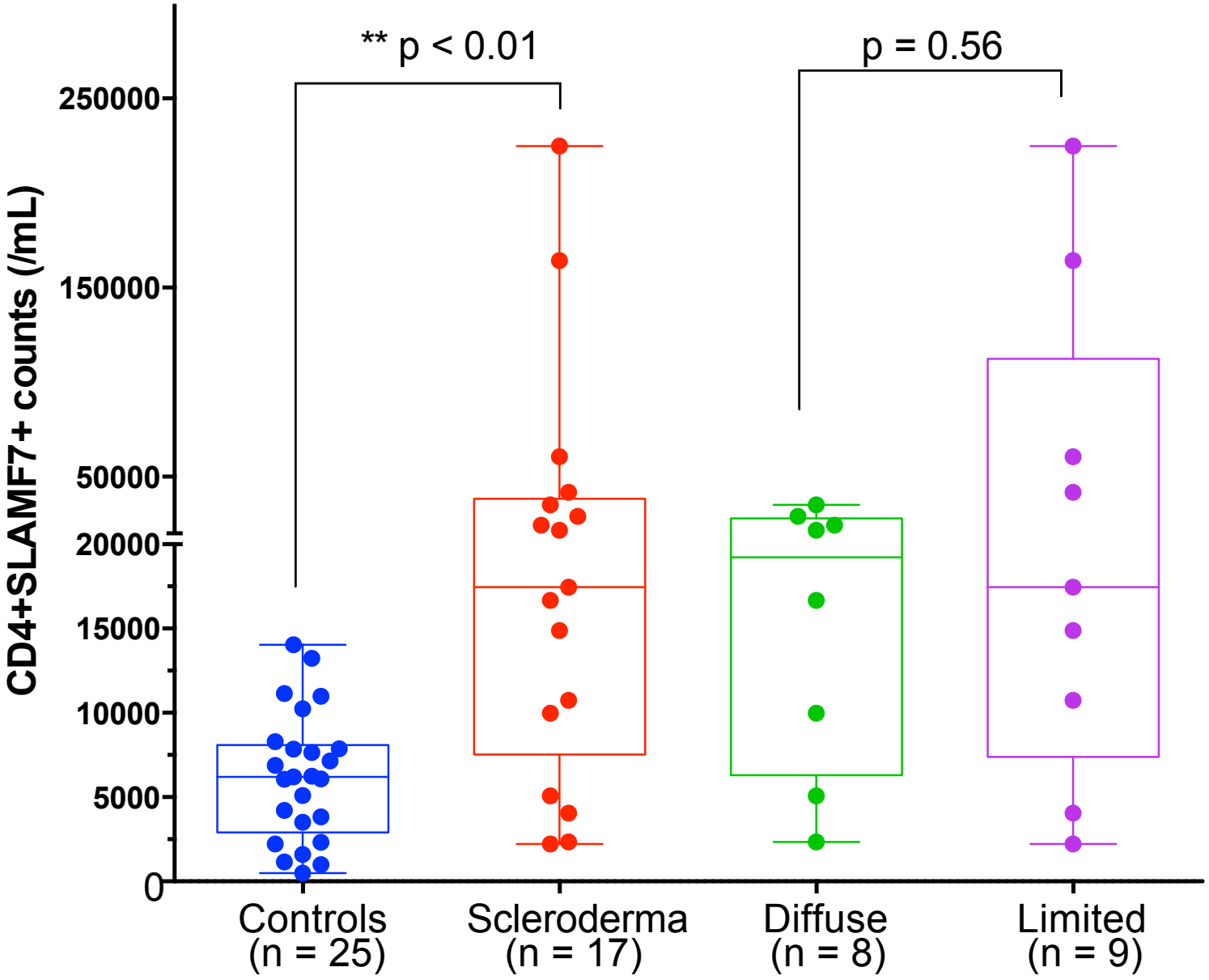
Subset Name	Median : Comp-FITC-A
CTLs	324
CD4+CD27+	448



Subset Name	Median : Comp-FITC-A
CTLs	429
CD4+CD27+	340



Subset Name	Median : Comp-FITC-A
CTLs	263
CD4+CD27+	455


** p < 0.01
p = 0.56
CD4+SLAMF7+ counts (/mL)
250000
150000
50000
20000
15000
10000
5000
0
Controls
(n = 25)
Scleroderma
(n = 17)
Diffuse
(n = 8)
Limited
(n = 9)